Biomaterials 257 (2020) 120250

Contents lists available at ScienceDirect

Biomaterials

journal homepage: www.elsevier.com/locate/biomaterials

Genetic engineering of novel super long-acting Exendin-4 chimeric protein for effective treatment of metabolic and cognitive complications of obesity

Jong Youl Lee [a,1], Taehoon Park [b,1], Eunmi Hong [c], Reeju Amatya [b], Kyung-Ah Park [a], Young-Hoon Park [c], Kyoung Ah Min [d], Minki Jin [d], Sumi Lee [d], Seungmi Hwang [d], Gu Seob Roh [a,**], Meong Cheol Shin [b,*]

[a] Department of Anatomy and Convergence Medical Science, Bio Anti-Aging Medical Research Center, Institute of Health Sciences, College of Medicine, Gyeongsang National University, Jinju, Gyeongnam, 52727, Republic of Korea
[b] College of Pharmacy and Research Institute of Pharmaceutical Sciences, Gyeongsang National University, 501 Jinju Daero, Jinju, Gyeongnam, 52828, Republic of Korea
[c] New Drug Development Center, Daegu-Gyeongbuk Medical Innovation Foundation (DGMIF), Daegu, 41061, Republic of Korea
[d] College of Pharmacy and Inje Institute of Pharmaceutical Sciences and Research, Inje University, Gimhae, Gyeongnam, 50834, Republic of Korea

ARTICLE INFO

Keywords:
Exendin-4
Albumin binding domain
FcRn
Affibody
GLP-1R
Obesity

ABSTRACT

A common bottleneck challenge for many therapeutic proteins lies in their short plasma half-lives, which often makes the treatment far less compliant or even disables achieving sufficient therapeutic efficacy. To address this problem, we introduce a novel drug delivery strategy based on the genetic fusion of an albumin binding domain (ABD) and an anti-neonatal Fc receptor (FcRn) affibody (AFF) to therapeutic proteins. This ABD-AFF fusion strategy can provide a synergistic effect on extending the plasma residence time by, on one hand, preventing the rapid glomerular filtration *via* ABD-mediated albumin binding and, on the other hand, increasing the efficiency of FcRn-mediated recycling by AFF-mediated high-affinity binding to the FcRn. In this research, we explored the feasibility of applying the ABD-AFF fusion strategy to exendin-4 (EX), a clinically available anti-diabetic peptide possessing a short plasma half-life. The EX-ABD-AFF produced from the *E. coli* displayed a remarkably (241-fold) longer plasma half-life than the SUMO tagged-EX (SUMO-EX) (0.7 h) in mice. Furthermore, in high-fat diet (HFD)-fed obese mice model, the EX-ABD-AFF could provide significant hypoglycemic effects for over 12 days, accompanied by a reduction of body weight. In the long-term study, the EX-ABD-AFF could significantly reverse the obesity-related metabolic complications (hyperglycemia, hyperlipidemia, and hepatic steatosis) and, moreover, improve cognitive deficits. Overall, this study demonstrated that the ABD-AFF fusion could be an effective strategy to greatly increase the plasma half-lives of therapeutic proteins and thus markedly improve their druggability.

1. Introduction

Exendin-4 (EX), a 39 amino acid peptide produced by the salivary glands of Gila monster (*Heloderma suspectum*), is aglucagon-like peptide-1 receptor (GLP-1R) agonist [1]. In 2005, a synthetic EX (trade name: Byetta®) was approved for the treatment of type 2 diabetes [2,3]. The therapeutic activities of the EX include 1) increase of glucose-dependent insulin synthesis and secretion, 2) inhibition of glucose-dependent glucagon secretion, 3) increase of gastric emptying time, 4) reduction of food intake and body weight, and 5) increase of pancreatic beta-cell mass and function [2]. In spite of its great efficacy in the treatment of diabetes, because of the small size (4.2 kDa), the EX experienced rapid clearance from the body and could exert therapeutic effects for only less than 12 h. Thus, to effectively control the blood glucose level, it was necessary to administer the EX twice daily [2]. To improve the patients' compliance, to date, many types of long-acting GLP-1R agonists have been developed [4–11]. Notably, some of them including Dulaglutide (a chemical conjugate of GLP-1 and the Fc region of IgG4) [12], and

* Corresponding author.
** Corresponding author.
E-mail addresses: anaroh@gnu.ac.kr (G.S. Roh), shinmc@gnu.ac.kr (M.C. Shin).
[1] Jong Youl Lee and Taehoon Park contributed equally to the manuscript.

https://doi.org/10.1016/j.biomaterials.2020.120250
Received 1 February 2020; Received in revised form 21 June 2020; Accepted 17 July 2020
Available online 21 July 2020
0142-9612/

Albiglutide (a fusion protein composed of GLP-1 dimer and a human albumin) [13] are clinically available. Yet, the plasma half-lives of the modified GLP-1R agonists were generally limited to less than 2 days (in mice) and their duration of therapeutic effects could be extended by no more than a week [4–11].

The elimination of administered therapeutic proteins occurs by various pathways including renal filtration, receptor-mediated clearance, and proteolytic metabolism [14–17]. Regarding the renal filtration, the protein size is the critical factor, as any protein with a size smaller than the albumin (66.5 kDa for human) would go through this clearance mechanism [16]. On the other hand, the receptor-mediated clearance occurs for many therapeutic proteins after binding to their target receptors or otherwise by internalization *via* pinocytosis [17]. Once internalized, these proteins would generally proceed to lysosomal degradation. Based on these clearance mechanism, various approaches have been attempted to prolong the blood circulation of therapeutic proteins [17–19]. Among them, specifically, exploiting the FcRn-mediated recycling has recently drawn great interest, because of its high efficiency.

FcRn is a major histocompatibility (MHC) class I-related heterodimeric protein residing primarily in the endosomal compartments of vascular endothelia and hematopoietic origin cells [20,21]. Specifically, the immunoglobulin G (IgG) and serum albumins could bind FcRn in a strictly pH-dependent manner [20,21]. They strongly bind to the FcRn at acidic pH but binds with less than 2 orders of magnitude at neutral pH [21]. This characteristic binding behavior allows the FcRn to protect the endocytosed IgG and albumin from lysosomal degradation (tight binding in acidic condition) and allow their recycling to the bloodstream (release in neutral pH). Fusion of the Fc part of IgG or albumin to therapeutic proteins could provide a direct approach for utilization of this FcRn-mediated recycling mechanism [20,21]. However, the molecular sizes of both the Fc part of IgG and albumin are relatively large (50 kDa and 66.5 kDa, respectively), which makes the fusion protein expression more difficult and less economic [22]. In this regard, the use of albumin binding domain (ABD) as a fusion partner could be a preferable option. The ABD is a group of small proteins that have specific binding affinity to albumin. Given the abundance of albumin in the plasma, the ABD is considered likely to instantly bind albumins after entering the bloodstream. The most widely adopted ABD is the albumin-binding protein domain GA148-GA3 from streptococcal protein G and its derivatives [23,24]. These ABD are relatively small (about 5 kDa), simple in their structure, and could be produced in *E. coli* with high yield. Therefore, they have been favorably utilized in many researches. However, there is a major limitation of the ABD and the albumin fusion strategy, which is the fact that the interaction between albumin and FcRn is relatively weak, compared with the IgG and the FcRn, which makes the ABD fusion protein less competent to compete for the FcRn binding with other endogenous albumins [23].

Affibodies are a class of small antibody mimetics which possess high specificity and affinity to their targets [25]. They are composed of only 58 amino acids and generally have no cysteine residues in their sequence, thus could be efficiently produced as fusion proteins by either genetic recombination or chemical conjugation with minimally affecting the intrinsic activity of the fusion partner [26]. Recently, Seijsing et al. reported the development of several anti-FcRn affibodies (AFF) which possess an extremely high binding affinity to the FcRn [22]. More

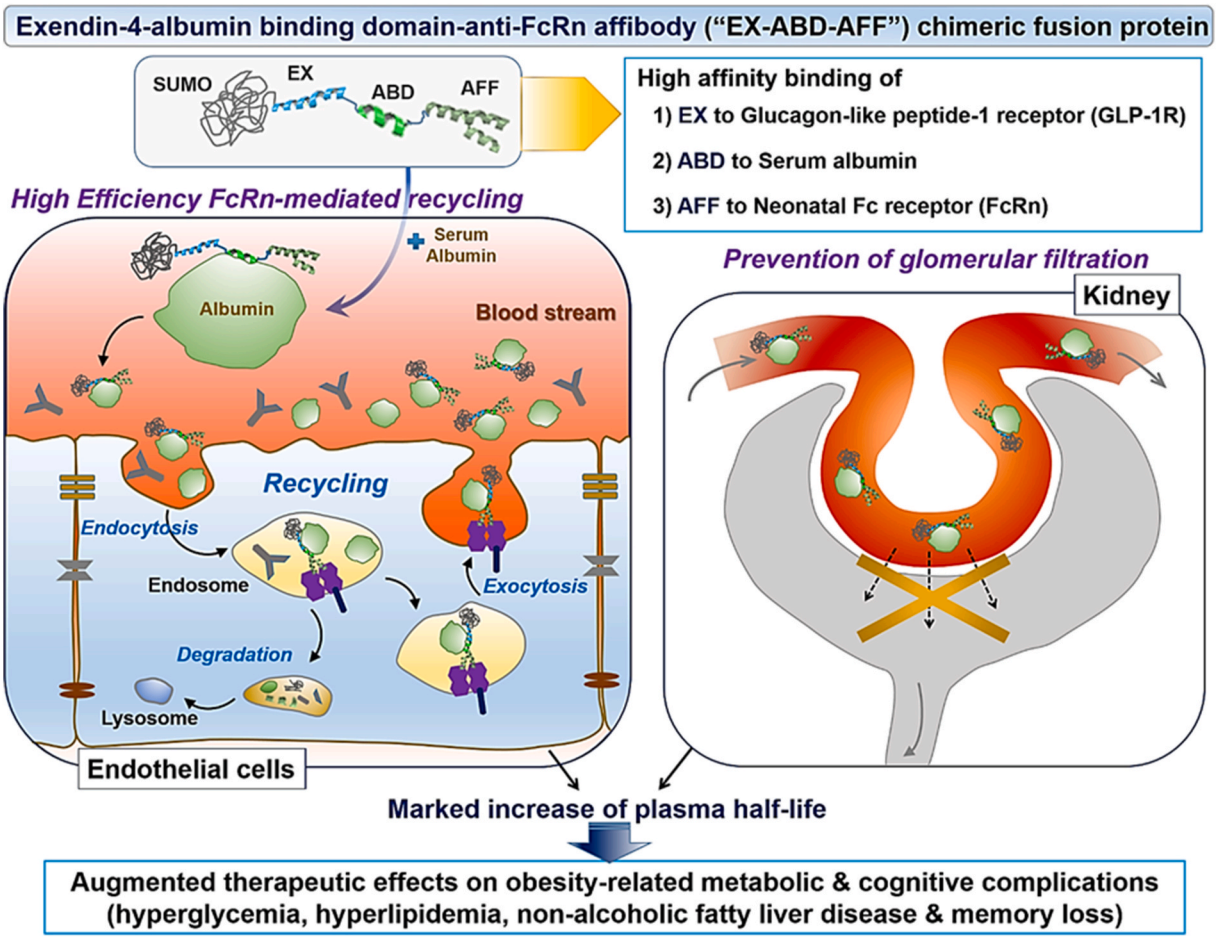

Fig. 1. Scheme of the drug delivery strategy devised for effective treatment of metabolic and cognitive complications of obesity by EX-ABD-AFF. (EX: exendin-4, ABD: albumin-bindind domain, AFF: anti-FcRn affibody).

interestingly, genetic fusion of ABD with these AFF could provide even synergistic effects on their binding to the FcRn, which led to more increased plasma half-lives of the ABD-AFF fusion proteins, compared with the ABD alone [22].

In this research, we genetically engineered a novel super long-acting EX fusion protein in which EX is fused in parallel with ABD and AFF. The scheme of the fusion protein and the drug delivery strategy (DDS) is depicted in Fig. 1. This EX-ABD-AFF showed a remarkable increase (7 days) in the plasma half-life compared to the SUMO-EX (0.7 h) in mice. Due to the prolonged plasma residence time, the EX-ABD-AFF could enable effective blood glucose control for over 12 days and, moreover, provide significant therapeutic effects on treatment of obesity-induced metabolic complications (hyperglycemia, hyperlipidemia, and non-alcoholic fatty liver disease (NAFLD)) and cognitive dysfunctions.

2. Materials and methods

2.1. Materials

Isopropyl-β-thiogalactopyranoside (IPTG) and LB broth were purchased from ThermoFisher Scientific (Waltham, MA, USA). Restriction endonucleases (*Nde*I & EcoRI) and T4 DNA ligase were purchased from New England Biolabs (Ipswich, MA, USA). Competent *Escherichia Coli* (E. *coli*) strains (DH5α and BL21 (DE3)) were purchased from Invitrogen (Carlsbad, CA, USA). Kanamycin was purchased from Sigma Aldrich (St. Louis, MO, USA). Exendin-4 peptide (EXp) was synthesized from Genscript Biotech (Piscataway, NJ, USA).

2.2. Preparation of SUMO-EX and EX-fusion proteins (EX-ABD, EX-AFF, and EX-ABD-AFF)

2.2.1. Construction of SUMO- EX and EX-fusion proteins' expression vectors

The genes encoding SUMO-EX (441 bp), EX-ABD (336 bp), EX-AFF (375 bp), and EX-ABD-AFF (570 bp) (Genscript Biotech) were double digested with restriction enzymes (*Nde*I & EcoRI) and then, after purification on 1% agarose gel, separately ligated into pET28a vector (for SUMO-EX) and pET28a-SUMO vector (in case of EX-ABD, EX-AFF, and EX-ABD-AFF). The constructed pET-SUMO-EX, pET-SUMO-EX-ABD, pET-SUMO-EX-AFF, and pET-SUMO-EX-ABD-AFF vectors were submitted for DNA sequencing analysis. In, addition, SUMO-EX fused with ABD and a control affibody ("EX-ABD-controlAFF") was prepared by following the identical procedures as above. The control AFF was prepared by adopting the anti-HER2 affibody (Z_{HER2}:342) gene sequence [27]. The schematic images of the expression vectors are shown in Fig. 2A and the protein sequences of EX, ABD, and AFF, control AFF are shown in Table 1.

2.2.2. Expression and purification of the SUMO-EX and EX-fusion proteins

For the production of SUMO-EX, a colony of BL21 (DE3) *E. coli* transformed with pET-SUMO-EX was picked and then used to inoculate 40 mL of LB medium (containing kanamycin 80 μg/mL). This starter culture was incubated at 37 °C (with shaking at 220 rpm) overnight and then diluted to 1 L LB medium (with kanamycin 80 μg/mL). The large culture was incubated under the same condition, and, when the optical density at 600 nm (OD_{600}) reached 1, IPTG was added to the final 0.5 mM to induce the production. The culture was further maintained under

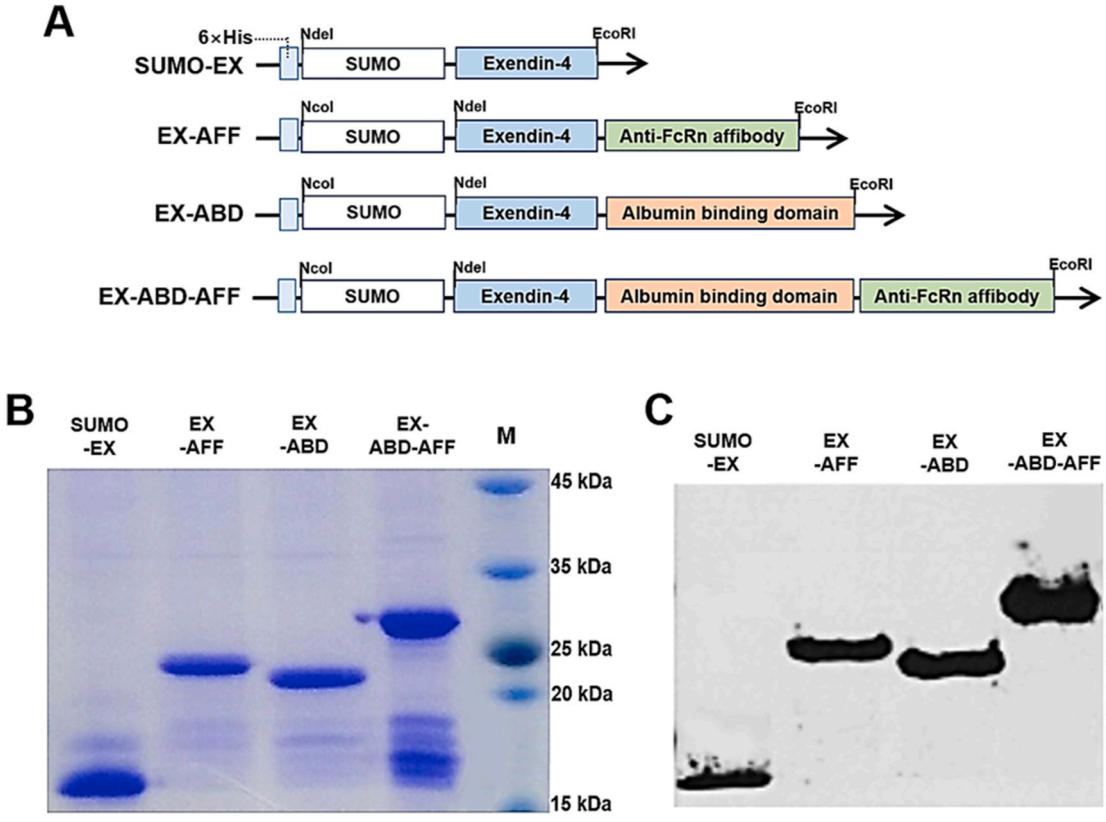

Fig. 2. Genetic engineering and production of SUMO-EX and EX-fusion proteins. (A) Schematic vector images, (B) SDS-PAGE, and (C) Western blot assay results for the expression of SUMO-EX, EX-AFF, EX-ABD, and EX-ABD-AFF from *E. coli*. The protein products purified by Talon metal affinity chromatography were loaded onto a 12% Tris-HCl SDS-PAGE gel, and the separated proteins were electroblotted on a nitrocellulose membrane. The expression of SUMO-EX and the EX-fusion proteins was identified with anti-His tag antibody. Lane M is a marker of the protein molecular weight standard (Invitrogen). (SUMO-EX: SUMO-tagged exendin-4, EX-AFF: SUMO-tagged exendin-4-anti-FcRn affibody fusion protein, EX-ABD: SUMO-tagged exendin-4-albumin binding domain fusion protein, and EX-ABD-AFF: SUMO-tagged exendin-4-albumin binding domain-anti-FcRn affibody fusion protein).

Table 1
Protein sequences of exendin-4 (EX), albumin binding domain (ABD), and anti-FcRn affibody (AFF).

Proteins	Protein sequences
EX (39 a.a.)	HGEGTFTSDLSKQMEEEAVRLFIEWLKNGGPSSGAPPPS
ABD (45 a.a.)	LKEAKEKAIEELKKAGITSDYYFDLINKAKTVEGVNALKDEILKA
AFF (58 a.a.)	VDAKYAKEFESAAHEIRWLPNLTYDQRVAFIHKLSDDPSQSSELLSEAKKLNDSQAPK
Control AFF (58 a.a.)	VDNKFNKEMRNAYWEIALLPNLNNQQKRAFIRSLYDDPSQSANLLAEAKKLNDAQAPK

the same condition for 4 h. After incubation, the *E. coli* cells were harvested by centrifugation and then re-dispersed in the PBS buffer (20 mM phosphate buffer with 300 mM NaCl, pH 7). The cells were lysed by sonication and, after centrifugation, the supernatant fraction was collected and the soluble SUMO-EX were purified from the impurities by applying the cell lysates to Talon resins (TALON Superflow resin, GE Healthcare Bio-Sciences, Pittsburgh, PA, USA). The expression and purification of EX-ABD, EX-AFF, EX-ABD-AFF, and EX-ABD-controlAFF were carried out by following the identical procedures for the production of the SUMO-EX. The final SUMO-EX and EX-fusion proteins were kept at 4 °C until further use.

2.2.3. Protein assays

Expression and purification of SUMO-EX and EX-fusion proteins were monitored by SDS-PAGE and western blotting. For the Western blot, the final products from Talon resin purification were electrophoresed on 12% Tris-HCl gel. Protein bands on the gel were transferred to a nitrocellulose membrane, and the membrane was blocked with 5% skim milk. After wash, the membrane was incubated with rabbit anti-6 × His tag antibody (1:1000 dilution; 2365S; Cell Signaling Technology, Danvers, MA, USA) at 4 °C overnight (o.n.). After wash, the membrane was then incubated with a secondary antibody (horseradish peroxidase-conjugated anti-rabbit IgG; 1:5000 dilution; CSB-PA564648; Cusabio Technology, Houston, TX, USA) at room temperature for 1.5 h. After another wash, the blots were developed. The yields and purities of the SUMOEX and EX-fusion proteins were determined by using BCA protein assay [28] and densitometry analysis (image J software from National Institutes of Health, Bethesda, MD, USA), respectively.

2.3. Surface plasmon resonance (SPR) assay

Kinetic analyses for the binding of EX-ABD-AFF to human GLP-1R, human serum albumin (HSA) and human FcRn (hFcRn) were conducted using Biacore T200 system (GE Healthcare Bio-Sciences, Pittsburgh, PA, USA). Based on the results, the association rate constants (k_a), dissociation rate constants (k_d) and the equilibrium dissociation (binding) constants (K_D; k_d/k_a) were determined.

2.3.1. Binding study of EX-ABD-AFF to GLP-1R

GLP-1R (10 μg/mL in 10 mM acetate buffer; pH 4.0; Abcam, Cambridge, MA, US) was immobilized onto a CM-5 sensor chip (GE Healthcare Bio-Sciences). Purified EX-ABD-AFF samples (7.8, 15.6, 31.3, 62.5, 125, and 500 nM) were prepared in PBS-P running buffer and injected at a constant flow rate of 30 μL/min. The contact time was set at 120 s and the dissociation time was at 1200 s.

2.3.2. Binding study of EX-ABD-AFF to HSA

HSA (0.25 μg/mL in 10 mM acetate buffer; pH 5.0; Sigma Aldrich) was immobilized onto the CM-5 sensor chip (GE Healthcare Bio-Sciences). Purified EX-ABD-AFF samples (15.625, 31.25, 62.5, 125, 250, 500, 1000, and 2000 nM) were prepared in PBS-P running buffer and injected at a constant flow rate of 30 μL/min. The contact time was set at 120 s and the dissociation time was at 1200 s.

2.3.3. Binding study of EX-ABD-AFF to hFcRn

The hFcRn (1 μg/mL in 10 mM acetate buffer; pH 4.5; R&D Systems, Inc., Minneapolis, MN, USA) was immobilized onto the CM-5 sensor chip (GE Healthcare Bio-Sciences). For testing at acidic condition, purified EX-ABD-AFF samples (15.625, 31.25, 62.5, 125, 500, 1000, 2000, and 5000 nM) were prepared in McIlvaine's phosphate-citrate running buffer (pH 6.0; 0.005% Tween 20) and injected at a constant flow rate of 30 μL/min. In case of neutral condition, the EX-ABD-AFF (15.625, 31.25, 62.5, 125, and 250 nM) were prepared in McIlvaine's phosphate-citrate running buffer (pH 7.4; 0.005% Tween 20). The contact time was set at 120 s and the dissociation time was at 1200 s.

2.4. GLP-1R activation assay

The GLP-1R activation potency of EXp, SUMO-EX and EX-fusion proteins were determined by using the PathHunter® GLP1 (7–37) Bioassay Kit (Eurofins DiscoverX Corporation, Fremont, CA, USA), following the manufacturer's protocol. This study is a cell-based assay using CHO–K1 cells co-expressing inactive β-galactosidase fragment fused to GLP-1R and β-Arrestin fused with N-terminal deletion mutant of β-gal. Activation of the GLP-1R stimulates the binding of β-Arrestin to the GLP-1R, which, in turn, leads to formation of an active β-gal. By measuring the β-gal activity *via* chemiluminescent assay, the GLP-1R activation could be identified. Briefly, the CHO–K1 cells were plated onto 96 well plates and incubated in the cell incubator for 48 h. After then, the cells were incubated with either 1) PBS, 2) EXp, 3) SUMO-EX, 4) EX-AFF, 5) EX-ABD, or 6) EX-ABD-AFF (N = 3) for 90 min. The concentration ranges for the assay were 10^{-12} – 10^{-5} M for EXp, and 10^{-12} – 5×10^{-4} M for SUMO-EX and EX-fusion proteins. After incubation, the cells were treated with detection reagents (1 and 2), and then the chemiluminiscence signal was measured by using the luminometer (TriStar LB 941, Berthold Technologies, Germany). The relative luminescence intensity (R.L.I.) was plotted against the sample concentrations, and the EC_{50} values for the samples were determined by using the Prism software (Prism version 8.0, GraphPad, San Diego, CA, USA).

2.5. Animal models

Male ICR and C57BL/6 mice (6 and 3 weeks old, respectively; KOATECH, Pyeongtaek, Republic of Korea) were housed in the animal facility at Gyeongsang National University (GNU). After arrival, the C57BL/6 mice were divided into two groups. One group of mice was fed with a normal chow diet (ND; 3.1 kcal/g; Harlan Laboratories, Inc., Indianapolis, IN, USA), while the other group of mice was on a high-fat diet (HFD; 60% kcal fat chow, 5.24 kcal/g, Research Diets, New Brunswick, NJ, USA). The body weights were measured weekly, and the blood glucose levels were measured every 3 weeks using an Accu-Chek glucometer (Roche Diagnostics GmbH, Mannheim, Germany). The short-term efficacy studies were carried out with the C57BL/6 mice, after 12 weeks of arrival when the bodyweight growth of the HFD-fed mice reached a plateau (bodyweight of HFD-fed mice: 43.8 ± 5.3 g; ND-fed mice: 28.3 ± 1.4 g). The long-term studies were initiated at week 16 (bodyweight of HFD-fed mice: 48.4 ± 1.9 g; ND-fed mice: 29.1 ± 1.4 g). The statistically significant difference of the bodyweights between the HFD- and ND-fed mice supported the establishment of the HFD-fed obesity model. All the experiments were performed in accordance with the study protocol approved by the University Animal Care Committee for Animal Research of Gyeongsang National University (GNU-160530-M0025).

2.6. Pharmacokinetic (PK) analyses

Male ICR mice were divided into −5 groups (N = 3) and, for 4 groups, subcutaneously (*s.c.*) administered with 50 nmol/kg of either: 1) SUMO-EX, 2) EX-AFF, 3) EX-ABD or 4) EX-ABD-AFF. The 5th group was administered with 50 nmol/kg of EX-ABD-AFF *via* tail vein injection. For the mice treated with SUMO-EX and EX-AFF, blood was withdrawn at 0, 5 min, 30 min, 1 h, 2 h, 4 h, 6 h, and 8 h post-administration. For the EX-ABD and EX-ABD-AFF, blood was withdrawn at 0, 10 min, 1 h, 3 h, 8 h, 1 day, 2 day, 3 day, 4 day, 7 day, 10 day, and 14 day post-administration. The blood was collected from the venous sinus using a capillary tube, and the plasma sample was acquired by centrifugation of the blood at 1000 rpm for 5 min. The concentrations of SUMO-EX and the EX-fusion proteins in the plasma samples were analyzed by ELISA using the EX enzyme immunoassay kit (EK-070-94, Phoenix Pharmaceuticals, Inc., Burlingame, CA), following the manufacturer's instruction. The PK profiles (plasma half-life, timepoint at which reached maximum concentration (T_{max}), maximum concentration (C_{max}), area under the curve (AUC), and mean residence time (MRT)) of the samples were determined by applying non-compartmental analysis to the plasma concentration-*vs*-time profiles using Phoenix® WinNonlin® software (Certara LP. Princeton, NJ, USA).

2.7. Biodistribution

Male C57/BL6 mice (6 weeks old) were administered with 50 nmol/kg of EX-ABD-AFF, and then at 1 day, 4 day, 7 day and 12 day of post-administration, the major organs (brain, pancreas, liver, heart, lung, spleen, intestine, and kidney) were harvested after euthalizing the mice (N = 5 for each time point). EX-ABD-AFF were extracted from the tissues, and then quantified by ELISA using the EX enzyme immunoassay kit (EK-070-94, Phoenix Pharmaceuticals, Inc.)

2.8. Glucose tolerance test (GTT)

GTT was carried out with the ND- and HFD-fed C57/BL6 mice, following the protocols described by Jeon et al. [29]. Briefly, the mice were divided into a total of 8 groups (N = 7): 1) ND + Saline, 2) HFD + Saline, 3) HFD + EXp (50 nmol/kg), 4) HFD + SUMO-EX (SUMO-EX 50 nmol/kg), 5) HFD + EX-ABD (EX-ABD 50 nmol/kg), 6) HFD + EX-AFF (EX-AFF 50 nmol/kg), 7) HFD + EX-ABD-AFF (EX-ABD-AFF 50 nmol/kg), and 8) HFD + EX-ABD-controlAFF (EX-ABD-controlAFF 50 nmol/kg). After fasting for 16 h, the mice were administered with the samples *via* intraperitoneal (*i.p.*) injection. One hour later, D-glucose (2 g/kg; Sigma-Aldrich, St. Louis, MO, USA) was injected (*i.p.*), and the blood glucose levels were measured at 0, 30, 60, 90, and 120 min post-administration using an Accu-Chek glucometer (Roche Diagnostics GmbH).

2.9. Short-term efficacy study for EX-fusion proteins by single administration in HFD-fed C57/BL6 mice

The HFD-fed C57/BL6 mice were divided into 9 groups (N = 7) and administered with either 1) saline, 2) EXp (200 nmol/kg), 3) SUMO-EX (50 nmol/kg), 4) SUMO-EX (200 nmol/kg), 5) EX-ABD (200 nmol/kg), 6) EX-AFF (200 nmol/kg), 7) EX-ABD-AFF (50 nmol/kg), 8) EX-ABD-AFF (200 nmol/kg) or 9) EX-ABD-controlAFF (200 nmol/kg) *via i.p.* injection. Total for 12 days after the treatment, the blood glucose level was measured at pre-determined time points (0, 1 h, 3 h, 6 h, 12 h, 1 day, 2 day, 3 day, 4 day, 5 day, 6 day, 7 day, and 12 day), and the body weights were monitored daily.

2.10. Evaluation of the therapeutic effects of EX-ABD-AFF on obesity-related metabolic complications and memory deficits after long-term (10-week) treatment

2.10.1. Animal treatment

The ND- and HFD-fed C57/BL6 mice were divided into 7 groups (N = 7): 1) ND + Saline, 2) ND + EX-ABD-AFF200 (EX-ABD-AFF 200 nmol/kg), 3) HFD + Saline, 4) HFD + SUMO-EX50 (SUMO-EX 50 nmol/kg), 5) HFD + SUMO-EX200 (SUMO-EX 200 nmol/kg), 6) HFD + EX-ABD-AFF50 (EX-ABD-AFF 50 nmol/kg), and 7) HFD + EX-ABD-AFF200 (EX-ABD-AFF 200 nmol/kg). The samples were administered *via i.p.* injection once per week for a total of 10 weeks. During the treatment, the blood glucose level, body weights, and the food intake amounts have been checked at a weekly base. After the 10 weeks of treatment, GTT and insulin tolerance test (ITT) were carried out with a 1-week interval. For the ITT, the mice were fasted 4 h prior to the study. After then, insulin (0.75 U/kg, Humulin-R, Eli Lilly, Indianapolis, IN, USA) was injected (*i.p.*), and the blood was collected at 0, 15, 30, 45, and 60 min-post administration. The glucose levels of the blood samples were measured.

2.10.2. Measurement of metabolic parameters and proinflammatory cytokine

After the 10-week treatment, the mice were fasted for overnight and deeply anesthetized with Zoletil (5 mg/kg; Virbac Laboratories, Carros, France). Blood was collected from the left ventricle and the serum samples were submitted for analyses of serum glucose, aspartate aminotransferase (AST) and alanine aminotransferase (ALT) (Green Cross Reference Laboratory, Yongin-si, Republic of Korea). The serum insulin were also measured using a plasma insulin ELISA kit (Shibayagi Co., Gunma, Japan).

2.10.3. Tissue collection and histologic examination

A group of mice (N = 4) were anesthetized with Zoletil and then perfused through the heart with heparinized saline followed by 4% paraformaldehyde in 0.1 M PBS. After fixation (6 h), the pancreases and livers were embedded in paraffin and then sliced into 5-μm tissue sections. The pancreas sections were stained with hematoxylin and eosin (H&E, Sigma-Aldrich), and the images of the sections were captured using a BX51 light microscope (Olympus, Tokyo, Japan). The percentage of pancreatic islet area was obtained from the selected images using i-Solution (IMT i-Solution Inc., Vancouver, BC, Canada). Three fields (150 × 150 μm^2) were randomly selected on each section from two continuous sections. For the liver samples, the deparaffinized liver sections were separately stained by H&E and Nile red and then visualized by light and fluorescence microscopy. In addition, histological analysis of H&E-stained liver sections (N = 3) was carried out to measure the NAFLD (non-alcoholic fatty liver disease) activity. The NAFLD activity score (NAS) was determined by summing the scores of steatosis (0–3), hepatocellular ballooning (0–2) and lobular inflammation (0–2).

2.10.4. Immunohistochemistry

Deparaffinized sections from pancreas were placed in a solution of 0.3% H_2O_2 for 10 min. After washing with 0.1 M PBS, the pancreas sections were treated with diluted blocking serum for 20 min, and then the slides were separately incubated overnight (o.n.) at 4 °C in a humidified chamber with rabbit anti-EX antibody (1:200 dilution; Bioss Inc., MA, USA), guinea pig anti-insulin antibody (1:100 dilution; Abcam, Cambridge, MA, USA), and rabbit anti-GLP-1R antibody (1:200 dilution; Abcam) diluted in blocking serum. After incubation, the sections were washed with PBS and incubated for 1 h at room temperature (RT) with secondary antibodies (1:200 dilution of either biotinylated goat anti-guinea pig antibody (Vector Laboratories, Burlingame, CA, USA) or horseradish peroxidase (HRP)-conjugated goat anti-rabbit antibody (ThermoFisher Scientific)). After washing, the biotinylated goat anti-guinea pig antibody-treated sections were incubated in avidin-biotin-peroxidase complex solution (ABC solution, Vector Laboratories).

After then, all the sections were developed with 0.05% diaminobenzidine (DAB, Vector Laboratories) containing 0.05% H_2O_2, and then dehydrated through graded alcohols, cleared in xylene, coverslipped with Permount (Sigma-Aldrich), and visualized under a BX51 light microscope (Olympus). Immunohistochemical intensity data for EX, insulin and GLP-1R were obtained from selected images using i-Solution (IMT i-Solution Inc.). Three fields (150 × 150 μm^2) were randomly selected on each section from two continuous sections. Intensity measurements are represented as the percentage of the mean number of pixels versus the corresponding value at which the pixel of the respective intensity was present.

2.10.5. Immunofluorescence

For double immunostaining, free-floating brain sections were incubated with rabbit anti-EX antibody (1:200 dilution, Bioss Inc.) and mouse GLP-1R antibody (1:100 dilution, Santa Cruz Biotechnology, CA, USA) at 4 °C for o.n. and washed. The brain sections were then incubated with donkey secondary antibodies conjugated with Alexa Fluor 488 (anti-rabbit) and 594 (anti-mouse) (Invitrogen, Carlsbad, USA), respectively. The fluorescence images of the sections were visualized under a BX51-DSU Olympus microscope.

2.10.6. Duolink immunofluorescence

To determine whether EX-ABD-AFF and GLP-1R were in sufficient proximity to interact in the hippocampus, the Duolink® in situ proximity ligation assay (PLA) from the OLINK Bioscience (Uppsala, Sweden) was carried out, according to the manufacturer's protocols. Briefly, the hippocampus sections were incubated with primary antibodies (mouse GLP-1R antibody (1:100 dilution, Santa Cruz Biotechnology), and rabbit anti-EX antibody (1:200 dilution, Bioss)). After washing, the section samples were incubated with PLA probes (anti-mouse MINUS (first PLA probe) and the anti-rabbit PLUS (second PLA probe)). After another wash, the section samples were ligated and amplificated. The hippocampus sections were then stained with DAPI, washed, and a coverslip was mounted using mounting medium. A negative control experiment was performed where only anti-EX antibody was added as the primary antibody. The fluorescent images of the sections were acquired by using a BX51-DSU Olympus microscope.

2.10.7. Western blot assay

After harvesting the mice brains, they were sequentially immersed in 15, 20, and 30% sucrose solution at 4 °C until they sank. After then, specifically, the hippocampus of the brains were collected and frozen. The frozen hippocampus was then homogenized in lysis buffer, and then the extracted proteins were immunoblotted with primary antibodies (for EX-ABD-AFF: 1:1000 dilution of mouse anti-6 × His tag Ab (ab18184), Abcam; for GLP-1R: 1:1000 dilution of rabbit anti-GLP-1R Ab (ab218532), Abcam). To normalize protein levels, β-actin (1:5000 dilution; T5168; mouse β-actin Ab, Sigma Aldrich) was used as the internal control. For the secondary antibody, horseradish peroxidase-conjugated goat anti-mouse or rabbit IgG (1:1,000, ThermoFisher Scientific) was used. Band densitometry analyses were carried out using the Multi-Gauge V 3.0 image analysis program (Fujifilm, Tokyo, Japan).

2.10.8. Morris Water Maze (MWM) test

The MWM test was conducted with the 10-week treated C57/BL6 mice (total 4 groups: ND + Saline, ND + EX-ABD-AFF200, HFD + Saline, and HFD + EX-ABD-AFF200) following the procedures described by Jeon et al. Briefly, for 4 consecutive days, the mice were trained to find a hidden platform (4 trials per day). The starting point was set to be different for each trial. After the 4 days of training, the probe test was performed on day 5. For the probe trials, the platform was removed and the mice were released in the center of the zone opposite of the previous platform quadrant. The mice were allowed to swim freely for 60 s, and their movements were recorded by a video-tracking program (Noldus EthoVision XT7, Noldus Information Technology, Netherlands).The time spent in the target zone where the platform was previously present during the training and the number of target zone crossings were measured.

2.11. Statistical analysis

All data were expressed as mean ± standard error of the mean (SEM). Statistical significant differences among groups were compared by using either 1-way ANOVA (with Tukey's multiple comparison test as post hoc test) or Student's t-test (Prism version 8.0, GraphPad). Results yielding $p < 0.05$ were considered statistically significant.

3. Results

3.1. Expression and purification of SUMO-EX and EX-fusion proteins

The SUMO-EX and EX-fusion proteins (EX-ABD, EX-AFF, and EX-ABD-AFF) were expressed as soluble SUMO-tagged proteins from *E. coli* and successfully purified by using Talon metal affinity chromatography (ThermoFisher Scientific). As shown in Fig. 2B, the final products after purification were clearly identified from the SDS-PAGE gel, and the theoretical protein sizes of SUMO-EX (17.9 kDa), EX-ABD (23.3 kDa), EX-AFF (24.9 kDa), and EX-ABD-AFF (31.2 kDa) were consistent with the band positions on the SDS-PAGE gel. The production of SUMO-EX and the EX-fusion proteins was further confirmed by the Western blot results (Fig. 2C). The average yields of SUMO-EX, EX-ABD, EX-AFF, and EX-ABD-AFF from 1 L culture were 22, 9.3, 8.7, and 16 mg, respectively, and the purities measured by densitometry analysis (image J software) were over 80%, except for EX-ABD-AFF (>70%). The SUMO-EX-ABD-controlAFF were also expressed as soluble SUMO-tagged fusion proteins and could be successfully purified by the Talon metal affinity chromatography (data not shown).

3.2. SPR assay results for binding of EX-ABD-AFF to GLP-1R, HSA, and hFcRn

The binding of EX-ABD-AFF with GLP-1R, HSA and hFcRn were characterized by biosensor analysis. The sensorgrams of the binding of EX-ABD-AFF to GLP-1R, HSA, and hFcRn are shown in Fig. S1 (supplementary data), and the association rate constants (k_a), the dissociation rate constants (k_d) and the overall affinities (K_D) are summarized in Table 2. As seen, the binding affinities for EX-ABD-AFF against all the tested counterpart proteins were found considerably high (K_D for GLP-1R, HSA, and hFcRn (at acidic condition; pH 6): 6.97×10^{-8}, 4.96×10^{-9}, and 8.32×10^{-8} M, respectively). However, the EX-ABD-AFF did not bind to hFcRn at neutral (pH 7.4) condition (Fig. S1D).

3.3. GLP-1R activation assay

As a GLP-1R agonist, the EX binding to the GLP-1R induces downstream signal transduction, and eventually leads to exocytosis of insulin from the pancreatic β cells. To determine the potency of the EXp, SUMO-EX and EX-fusion proteins for activating the GLP-1R, a cell-based study

Table 2
Summary of the binding affinities of EX-ABD-AFF to glucagon-like peptide-1 receptor (GLP-1R), human serum albumin (HSA) and human neonatal Fc receptor (hFcRn).

Parameters	GLP-1R	HSA	hFcRn
k_a (1/Ms)	$6.12x10^4$	$4.40x10^4$	$1.16x10^4$
k_d (1/s)	$4.27x10^{-3}$	$2.18x10^{-4}$	$9.64x10^{-4}$
K_D (M)	$6.97x10^{-8}$	$4.96x10^{-9}$	$8.32x10^{-8}$

EX-ABD-AFF: exendin-4-albumin binding domain-anti-FcRn affibody fusion, k_a: association rate constant, k_d: dissociation rate constant, and K_D (k_d/k_a): equilibrium dissociation (binding) constant (overall binding affinity).

using GLP-1R expressing CHO–K1 cells were carried out. As shown in Fig. S2, the SUMO-EX and EX-fusion proteins showed similar profiles, but their potencies were significantly lower than that of the EXp. The EC_{50} values for the GLP-1R activation were 3.2×10^{-9}, 1.2×10^{-5}, 1.3×10^{-5}, 1.2×10^{-5}, and 1.6×10^{-5} M for EXp, SUMO-EX, EX-ABD, EX-AFF, and EX-ABD-AFF, respectively.

3.4. PK profile analyses

The plasma concentration-versus-time curves of SUMO-EX and the EX-fusion proteins are shown in Fig. 3A–C, and the PK parameters are summarized in Table 3. As seen in Fig. 3A, the EX-AFF (*s.c.*) showed a 2-fold higher plasma half-life (1.5 h) with 5.5-fold higher AUC and 2.8-fold longer MRT than the SUMO-EX (*s.c.*). In the case of EX-ABD and EX-ABD-AFF, they exhibited a more markedly different PK profiles than the SUMO-EX (Fig. 3B). The EX-ABD (*s.c.*) showed a plasma half-life of 3.5 days with 163-fold higher AUC and 131-fold longer MRT, in comparison with SUMO-EX. For EX-ABD-AFF (*s.c.*), it showed an even longer plasma half-life of 7 days, and its AUC and MRT were 5.1-fold and 2.2-fold greater than those of the EX-ABD (compared with the SUMO-EX, the AUC and MRT were increased 821-fold and 293-fold, respectively). When the EX-ABD-AFF was administered by tail vein injection (*i.v.* bolus), in the plasma concentration-versus-time profile, the terminal phase closely resembled that of the EX-ABD-AFF (*s.c.*) (Fig. 3C). The plasma half-life (6 days) and the MRT (8 days) of EX-ABD-AFF (*i.v.*) were slightly shorter than those of the EX-ABD-AFF (*s.c.*), but the C_{max} and AUC were 2.5-fold and 1.1-fold higher.

3.5. Biodistribution

The tissue distribution profiles of EX-ABD-AFF are shown in Figs. 3D and S3. As seen, the EX-ABD-AFF was observed up to 12 days in most of the major organs. High levels of EX-ABD-AFF were observed in heart, lung and spleen, while only minimal amounts were found in the kidney (Fig. S3). Notably, a traceable amount of EX-ABD-AFF was observed from the main tissues of action (brain, pancreas, and liver) along the 12 days (Fig. 3D).

Table 3
Summary of the pharmacokinetic (PK) profiles of EX, EX-AFF, EX-ABD, and EX-ABD-AFF by *s.c.* injection and EX-ABD-AFF by *i.v.* bolus injection in ICR mice.

PK Parameters	EX (*s.c.*)	EX-AFF (*s.c.*)	EX-ABD (*s.c.*)	EX-ABD-AFF (*s.c.*)	EX-ABD-AFF (*i.v.* bolus)
Half-life ($t_{1/2}$; h)	0.69 (±0.04)[a]	1.50 (±0.05)	84.02 (**3.5 days**) (±11.09)	166.4 (**7 days**) (±4.12)	140.2 (**6 days**) (±7.62)
T_{max} (h)	0.083	0.5	1	3	–
C_{max} (ng/mL)	822.3 (±60.88)	1871 (±35.05)	4593 (±46.44)	5486 (±370.3)	13,997[b] (±2699)
$AUC_{0-\infty}$ (h·ng/mL)	606.6 (±6.43)	3361 (±144.9)	98,579 (±1847)	498,099 (±26,402)	542,508 (±6559)
MRT (h)	0.72 (±0.04)	2.02 (±0.10)	94.63 (**4 days**) (±3.82)	210.6 (**9 days**) (±3.53)	185.9 (**8 days**) (±2.17)

EX: exendin-4, EX-AFF: exendin-4-anti-FcRn affibody fusion, EX-ABD: exendin-4-albumin binding domain fusion, EX-ABD-AFF: exendin-4-albumin binding domain-anti-FcRn affibody fusion, T_{max}: timepoint at which reached maximum concentration, C_{max}: maximum concentration, AUC: area under the curve, and MRT: mean residence time.
[a] Standard error values of mean were exhibited in the parenthesis.
[b] For *i.v.* bolus injection of EX-ABD-AFF, the initial plasma concentration, Co (ng/mL) was displayed.

3.6. GTT assay

As shown in Fig. 4A, the GTT results showed that, in HFD-fed C57BL/

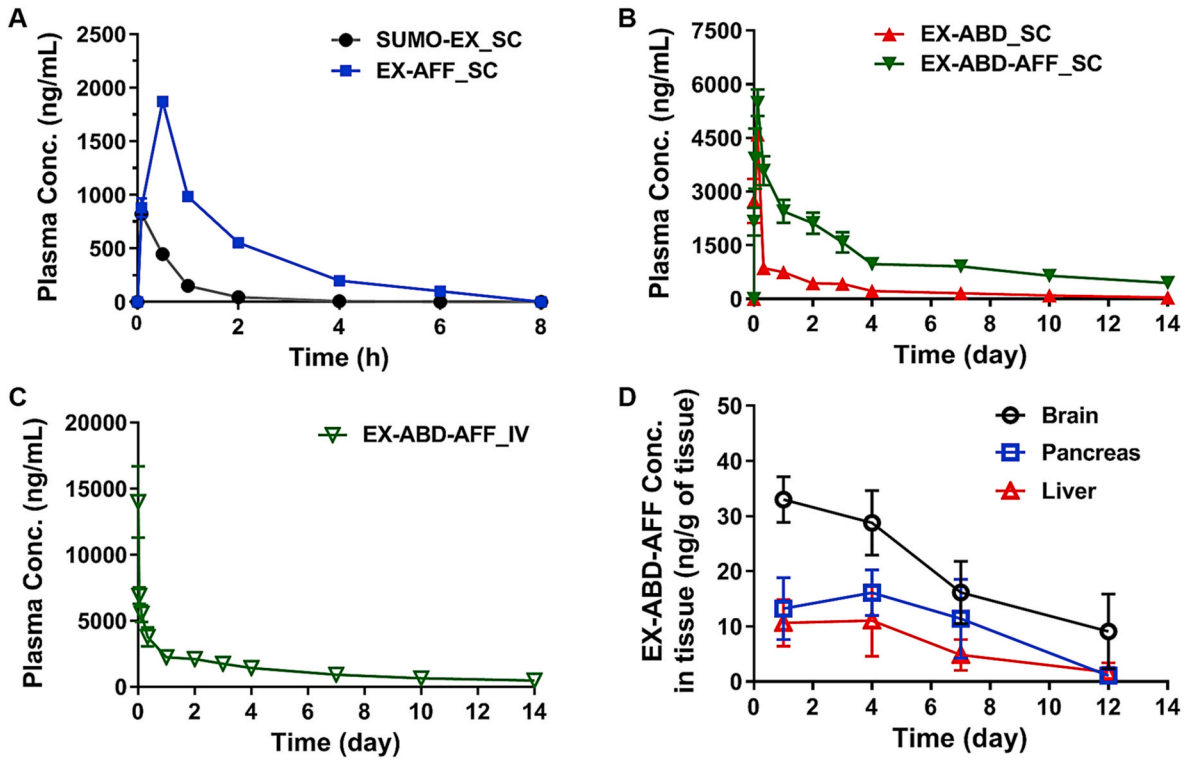

Fig. 3. Plasma concentration-versus-time profiles of subcutaneously (*s.c.*) administered (A) SUMO-EX and EX-AFF, (B) EX-ABD and EX-ABD-AFF, (C) intravenously (*i.v.*) administered EX-ABD-AFF in ICR mice, and (D) the biodistribution profiles of EX-ABD-AFF in the brain, pancreas and liver of C57/BL6 mice. (SUMO-EX: SUMO-tagged exendin-4, EX-AFF: SUMO-tagged exendin-4-anti-FcRn affibody fusion protein, EX-ABD: SUMO-tagged exendin-4-albumin binding domain fusion protein, and EX-ABD-AFF: SUMO-tagged exendin-4-albumin binding domain-anti-FcRn affibody fusion protein).

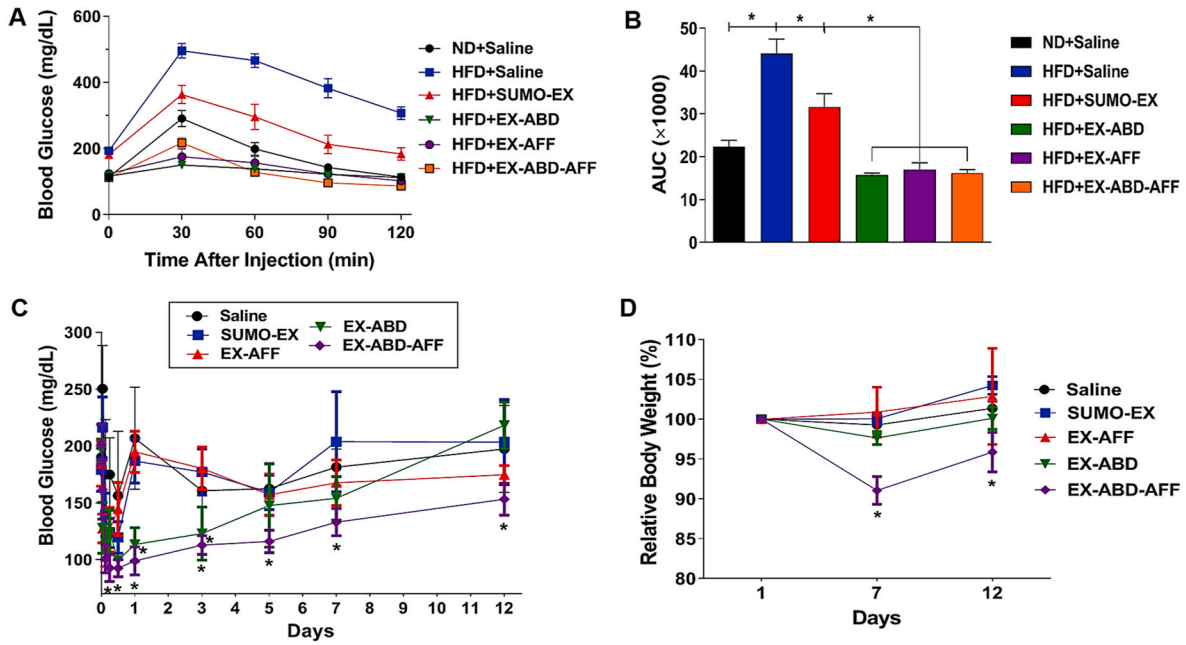

Fig. 4. Glucose tolerance test (GTT) and short-term efficacy study results for SUMO-EX, EX-AFF, EX-ABD, and EX-ABD-AFF by single administration in C57/BL6 mice. (A) Serum glucose levels of the mice after intraperitoneal administration of EX samples during the GTT assay. (B) Area under the curve (AUC) for the GTT results. (C) Blood glucose level-versus-time profiles, and (D) bodyweight changes of the HFD-fed mice during the efficacy study of the HFD-fed mice after intraperitoneal administration of different EX samples at 200 nmol/kg. The statistically significant difference in the body weight changes among the groups was compared by 1-way ANOVA and post hoc Tukey's multiple comparison test. *P < 0.05. (SUMO-EX: SUMO-tagged exendin-4, EX-AFF: SUMO-tagged exendin-4-anti-FcRn affibody fusion protein, EX-ABD: SUMO-tagged exendin-4-albumin binding domain fusion protein, and EX-ABD-AFF: SUMO-tagged exendin-4-albumin binding domain-anti-FcRn affibody fusion protein).

6 mice, SUMO-EX, EX-ABD, EX-AFF, and EX-ABD-AFF could all significantly prevent the increase of blood glucose level after the glucose load. Based on the AUC values, compared with SUMO-EX, the EX-fusion proteins showed more than 50% greater improvement in glucose tolerance (Fig. 4B). In addition, as seen in Fig. S4A, when the GTT results were compared among EXp, SUMO-EX, EX-ABD-controlAFF, and EX-ABD-AFF, the EXp and EX-ABD-AFF showed similar levels of improvement in the glucose tolerance. However, the SUMO-EX and EX-ABD-controlAFF exhibited lower effects, compared with the EXp.

3.7. Hypoglycemic effects and body weight loss by single administration of EX-fusion proteins in HFD-fed C57BL/6 mice

As shown in Fig. 4C, the blood glucose levels of the HFD-fed C57BL/6 mice administered with SUMO-EX and EX-fusion proteins were all significantly lower than that of the control mice for the first 6 h. However, while the hypoglycemic effects lasted less than a day for both SUMO-EX and EX-AFF, the EX-ABD and EX-ABD-AFF groups showed extended hypoglycemic effects with maintaining significantly lower blood glucose levels than the control mice for 3 and 12 days, respectively. When the hypoglycemic effects were compared among EXp, SUMO-EX, EX-ABD-controlAFF, and EX-ABD-AFF, the duration of the effects by EXp and SUMO-EX were similarly less than 12 h. However, the EX-ABD-controlAFF and the EX-ABD-AFF were found significantly effective for 3 and 12 days, respectively (Fig. S4B). The hypoglycemic effects of SUMO-EX and EX-ABD-AFF appeared dose-dependent (Fig. S4C). As seen in Fig. 4D, when the body weights of the HFD-fed mice were monitored during the study at days 1, 7 and 12, the saline, SUMO-EX and EX-AFF-treated groups showed a continual increase. In sharp comparison, for EX-ABD and EX-ABD-AFF-treated groups, weight loss was commonly observed on day 7. Specifically, the EX-ABD-AFF-treated mice showed significant weight loss, and this effect was also found dose-dependent (Fig. S4D).

3.8. Therapeutic effects of the long-term (10-week) treatment of EX-ABD-AFF on obesity-related metabolic and cognitive complications

3.8.1. Hypoglycemic effects of EX-ABD-AFF

After 16 weeks of arrival, the ND- and HFD-fed C57BL/6 mice have been treated once weekly for a total of 10 weeks with either SUMO-EX or EX-ABD-AFF, at doses of 50 or 200 nmol/kg. During the 10 weeks of study, both the SUMO-EX and EX-ABD-AFF treatments were well tolerated by all the ND- and HFD-fed mice. The weekly measurements of fasting blood glucose levels are shown in Fig. 5A. In addition, the serum glucose levels after termination of the 10-week treatment are shown in Fig. 5B. As seen, the fasting blood glucose level of the HFD + Saline mice was continuously maintained higher than that of the ND + Saline mice. Furthermore, the serum glucose levels of most of the HFD-fed groups were found over 250 mg/dL; indicating the presence of hyperglycemia in the HFD-fed mice. In these HFD-fed mice, the EX-ABD-AFF elicited dose-dependent hypoglycemic effects continuously during the treatment. Moreover, after the 10-week treatment, the HFD + EX-ABD-AFF200 group (244.0 mg/dL) showed significantly lower blood glucose level than the HFD control group (403.4 mg/dL). However, there was no significant difference in the blood glucose levels between the ND + EX-ABD-AFF200 group (170.1 mg/dL) and the ND + Saline group (235.9 mg/dL).

After termination of the study at week 10, GTT and ITT were also carried out. As shown in Figs. S5A and S5B, the glucose tolerance was found improved in the groups of HFD + EX-ABD-AFF50 and HFD + EX-ABD-AFF200 (average of 22 and 35% decreases of AUC, respectively), compared with the HFD + Saline mice. Based on the ITT results, compared with HFD + Saline, the insulin resistance was also found significantly improved in the groups of HFD + SUMO-EX200, HFD + EX-ABD-AFF50, and HFD + EX-ABD-AFF200 (average of 14.4, 17, and 20.1% decreases of AUC, respectively) (Figs. S5C and S5D).

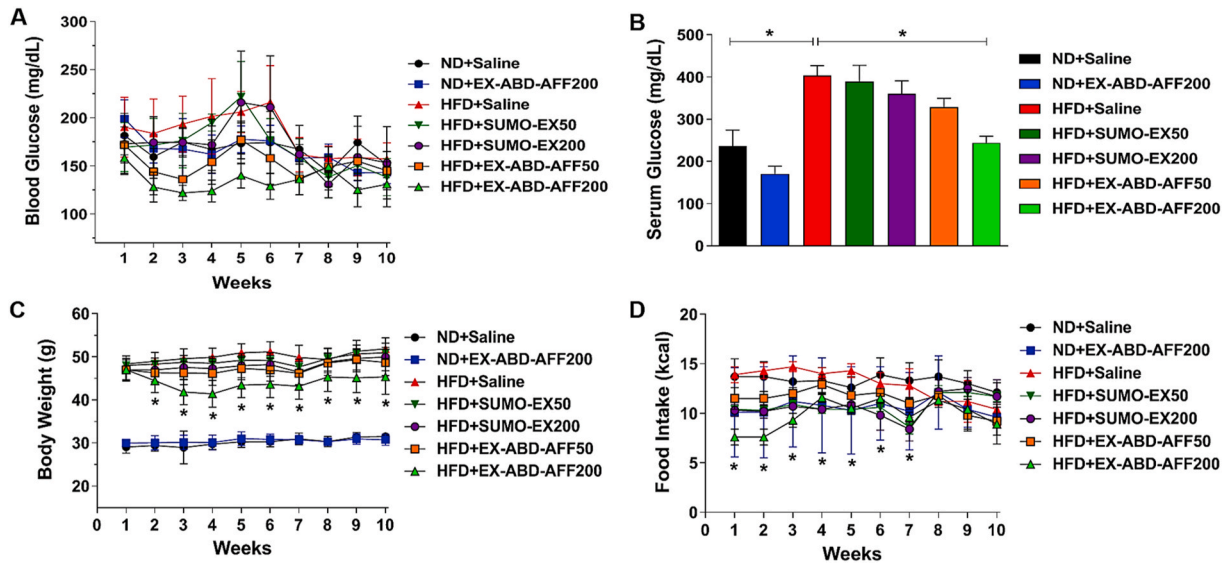

Fig. 5. Hypoglycemic effects and body weight loss by long-term (10 weeks) treatment of EX-ABD-AFF in high-fat diet (HFD)-fed C57/BL6 mice. (A) Fasting blood glucose levels over time and (B) serum glucose level (fasting) at the end of 10-week treatment. Weekly change of (C) body weights, and (D) food intake amounts over time. The statistically significant difference in the body weight changes among the groups was compared by 1-way ANOVA and post hoc Tukey's multiple comparison test. *P < 0.05. (SUMO-EX: SUMO-tagged exendin-4, EX-ABD-AFF: SUMO-tagged exendin-4-albumin binding domain-anti-FcRn affibody fusion protein).

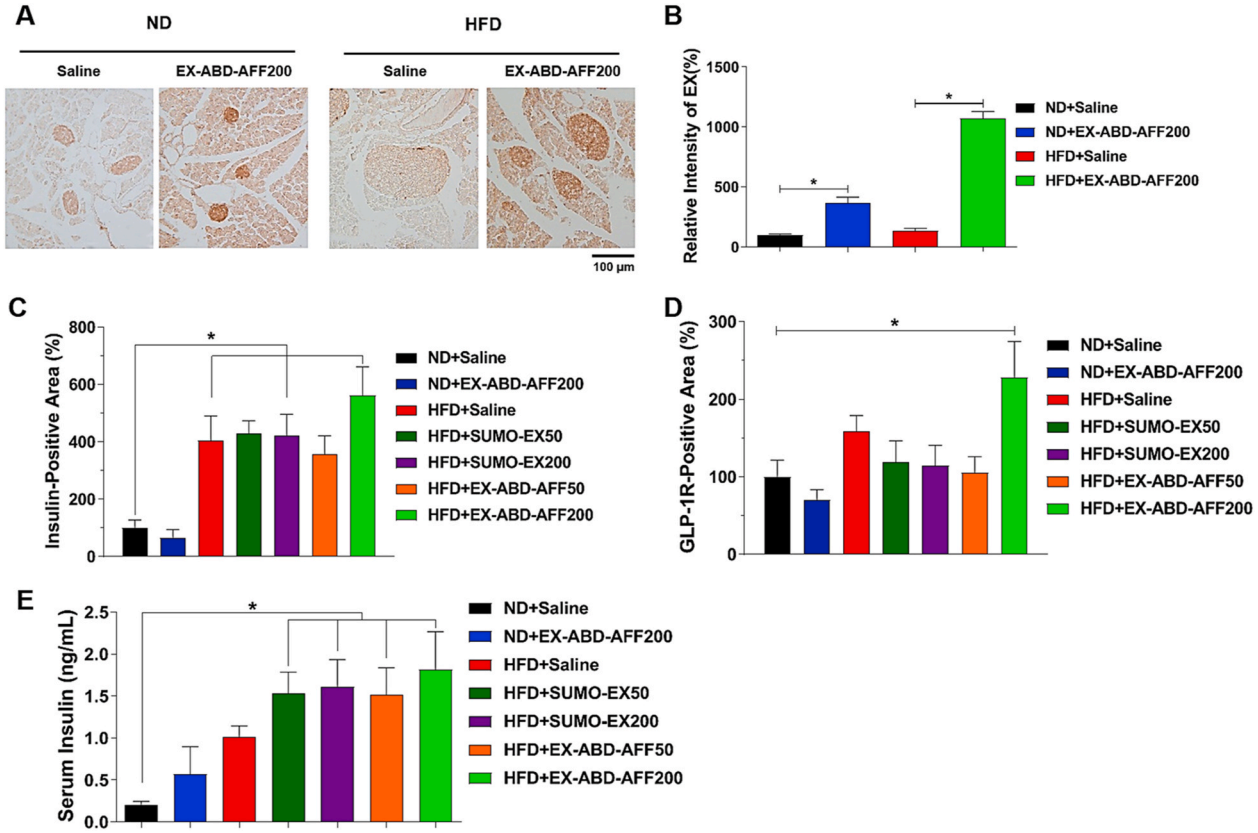

Fig. 6. Insulinotropic effects by long-term (10-week) treatment of EX-ABD-AFF in high-fat diet (HFD)-fed C57/BL6 mice. (A) Representative microscopic images of pancreatic sections stained with anti-exendin-4 antibody. (B) The relative intensity of the stained area was calculated by imaging analysis using i-Solution (IMT i-Solution Inc.). The pancreatic sections were also stained with H&E, anti-insulin antibody, or anti-GLP-1R antibody (The representative microscopic images of the pancreatic sections are shown in Fig. S6). From the stained pancreatic sections, (C) insulin-positive area (%), and (D) GLP-1R-positive area (%) were calculated by using i-Solution (IMT i-Solution Inc.). (E) Serum insulin levels measured after the 10-week treatment. The statistically significant difference in the body weight changes among the groups was compared by 1-way ANOVA and post hoc Tukey's multiple comparison test. *P < 0.05. (SUMO-EX: SUMO-tagged exendin-4, EX-ABD-AFF: SUMO-tagged exendin-4-albumin binding domain-anti-FcRn affibody fusion protein).

3.8.2. Effects of EX-ABD-AFF on body weight and food intake

The profiles of body weights and food intake amounts during the long-term efficacy study are summarized in Fig. 5C and D. As shown in Fig. 5C, both the ND + Saline and the HFD + Saline mice gradually gained weight from average 29.1 g–31.5 g (+2.4 g) and 48.4 g–51.8 g (+3.4 g), respectively. When compared with the ND + Saline group, the ND + EX-ABD-AFF200 group did not show loss but gained less weight (+0.8 g; 30 g–30.8 g) after the 10-week period. Among the HFD-fed mice, the HFD + Saline, HFD + SUMO-EX50, HFD + SUMO-EX200, and HFD + EX-ABD-AFF50 groups showed similarly increasing profiles of body weights. However, the mice in HFD + EX-ABD-AFF200 group displayed significantly reduced body weight during weeks 2–10. Compared with HFD + Saline, the bodyweight of HFD + EX-ABD-AFF200 group showed the highest (−17%) difference at week 4 and remained significantly lower (−13%) than that of the HFD + Saline by the end of the study.

As shown from Fig. 5D, the ND + Saline and the HFD + Saline mice showed similar amounts of weekly food intake (ND + Saline: 13.3 ± 0.6 kcal *vs.* HFD + Saline: 13.0 ± 1.5 kcal) throughout the study. Compared with the ND + Saline, the ND + EX-ABD-AFF200 group showed less food intake amounts (10.6 ± 0.7 kcal), but there was no statistical difference. In the case of the HFD-fed mice, HFD + SUMO-EX50, HFD + SUMO-EX200, HFD + EX-ABD-AFF50, and HFD + EX-ABD-AFF200 groups all showed significantly lower levels of food intake than the HFD + Saline during the first 7 weeks of treatment. Among them, the HFD + EX-ABD-AFF200 group showed the highest reduction in food intake (9.8 ± 1.5 kcal).

3.8.3. Insulinotropic effects of EX-ABD-AFF

To verify the insulinotropic activity of EX-ABD-AFF, after the 10-week treatment, the pancreas was harvested, and the tissue sections were separately stained with anti-EX antibody, H&E, anti-insulin antibody, and anti-GLP-1R antibody. The images of stained pancreas tissue sections are shown in Figs. 6A and S6, and the image analyses data for relative intensity of EX, insulin-positive area (%), and GLP-1R positive area (%) are exhibited in Fig. 6B–D. In addition, the average serum insulin levels are compared in Fig. 6E. Based on the histological analyses, first of all, the delivery of EX-ABD-AFF to the β cells was clearly identified from both ND and HFD-fed mice (Fig. 6A and B). Next, compared with ND + Saline mice, all the HFD groups commonly showed an increase in pancreatic islet area, insulin-positive area, and GLP-1R positive area (Fig. S6, Fig. 6C and D). These results indicated the presence of a typical β-cell hypertrophy and hyperplasia, caused by adaptation of the pancreas to the HFD-induced insulin resistance. Consistently, as shown in Fig. 6E, the serum insulin levels were also elevated in all the HFD-fed mice. However, among them, specifically, the HFD + EX-ABD-AFF200 group showed the highest increase (8.9-fold) in the serum insulin level as well as the most prominent enlargement in the sizes of β cells; evidencing the insulinotropic effects by the EX-ABD-AFF200.

3.8.4. Hypolipidemic activity of EX-ABD-AFF

After the 10-week treatment, epididymal fats, perirenal fats, and intestinal mesenteric fats were harvested from the mice and weighed. In addition, whole blood was drawn, and the serum samples were analyzed for FFA, total cholesterol and TG concentrations. These analyses data are shown in Fig. S7. As seen in Figs. S7A–S7B, the weights of total fats of the HFD-fed mice were about −2.3 – 3 times higher than those of the ND + Salinemice. The fat weights of ND + Saline group and ND + EX-ABD-AFF200 group showed little difference. Also, compared with the HFD + Saline group, HFD + SUMO-EX50, HFD + SUMO-EX200, and HFD + EX-ABD-AFF50 groups did not show significant decreases in the fat weights. However, in the case of HFD + EX-ABD-AFF200 group, the total fat weights (6.28 ± 1.0 g) were significantly lower than those of the HFD + Saline group (8.23 ± 3.0 g).

The serum fat-related data are shown in Figs. S7C–S7E. As seen, the serum FFA and TG values did not show differences between the ND + Saline and HFD + Saline groups, but the serum cholesterol level of the HFD + Saline group was 2.5-fold higher than that of the ND + Saline mice. In the ND mice, the EX-ABD-AFF treatment had no lowering effects for serum FFA, serum TG, and serum cholesterol levels. However, compared with the HFD + Saline group, a significant reduction of serum FFA and serum cholesterol levels were observed from the HFD + EX-ABD-AFF groups. For HFD + Saline, HFD + EX-ABD-AFF50, and HFD + EX-ABD-AFF200, serum FFA concentrations were 775.8, 533.5, and 529.9 μEq/L, respectively, and the serum cholesterol levels were 244.7, 189.2, and 169 mg/dL, respectively.

3.8.5. Amelioration of NAFLD by EX-ABD-AFF

NAFLD is a type of liver disease characterized by excessive fat accumulation in the liver without significant alcohol consumption [30]. To assess the effects of EX-ABD-AFF on the NAFLD in the HFD mice, after the 10-week treatment, livers were harvested from the mice, weighed and then fixed. Liver sections were prepared and separately stained with H&E and Nile red. Based on the stained liver images, NAFLD activity scores (NAS) were calculated. In addition, the concentrations of liver function markers (AST and ALT) in the blood samples were analyzed. These data are summarized in Figs. 7 and S8.

As shown in Fig. 7A, hepatic steatosis (fat accumulation in the liver) was clearly observed from the liver sections of HFD-fed mice (fats stained in red color by Nile red), but not from those of the ND-fed mice. Compared with HFD + Saline, the SUMO-EX-treated HFD groups showed no differences in the Nile red-stained liver images. However, the EX-ABD-AFF-treated HFD groups exhibited less accumulation of fat in the liver. Moreover, for steatosis, inflammation, ballooning, and the overall NAS all indicated significant improvement in the NAFLD conditions in EX-ABD-AFF-treated HFD mice (Fig. 7B and C). In good accordance, the blood analysis data showed a significant reduction of serum AST and ALT levels by the treatment of EX-ABD-AFF (Fig. 7D and E).

In addition, as seen from Fig. S8, when compared the appearance of the livers among the groups, the livers of the HFD + Saline mice were lighter in color and found enlarged with significantly increased (2-fold) weights (2.52 ± 0.3 g), compared with those of the ND-fed mice (1.22 ± 0.2 g). The livers of the SUMO-EX-treated HFD mice showed no clear difference in their appearance, and the liver weights were similar or slightly lower than those of the HFD + Saline mice (HFD + SUMO-EX50 and HFD + SUMO-EX200: 2.55 ± 0.3 g and 2.24 ± 0.3 g, respectively). In a sharp contrast, the morphology of the livers of EX-ABD-AFF-treated mice looked closer to those of the ND + Saline mice, and the liver weights (HFD + EX-ABD-AFF50 and HFD + EX-ABD-AFF200: 1.89 ± 0.3 g and 1.48 ± 0.2 g, respectively) were also significantly reduced close to those of the ND + Saline mice.

3.8.6. Improvement of cognitive deficits by EX-ABD-AFF

The therapeutic effects of the EX-ABD-AFF on cognitive deficits were evaluated in the 10-week treated mice by MWM test. The MWM test, reported by Richard G. Morris in 1984, is one of the most widely adopted behavioral tests for investigating hippocampal-dependent spatial learning and memory [31]. The representative swimming trajectories of the mice recorded during the 60 s of probe test in the MWM test are shown in Fig. 8A, and the average time spent in target quadrant zone and the average number of target zone crossings for the tested mice are exhibited in Fig. 8B and C, respectively. As seen, the MWM test results showed a clear difference in the behavior of the HFD + Saline and the ND + Saline groups. The swimming trajectories of the HFD + Saline mice displayed less directed movements toward the target quadrant than the ND + Saline mice. Accordingly, the time in the target quadrant zone and the numbers of target zone crossings were also significantly reduced in the HFD + Saline mice. Collectively, these results confirmed the presence of cognitive deficits in the HFD + Saline mice. This behavioral difference was, however, reversed in HFD + EX-ABD-AFF200 mice.

To verify whether this memory improvement is a direct action by EX-

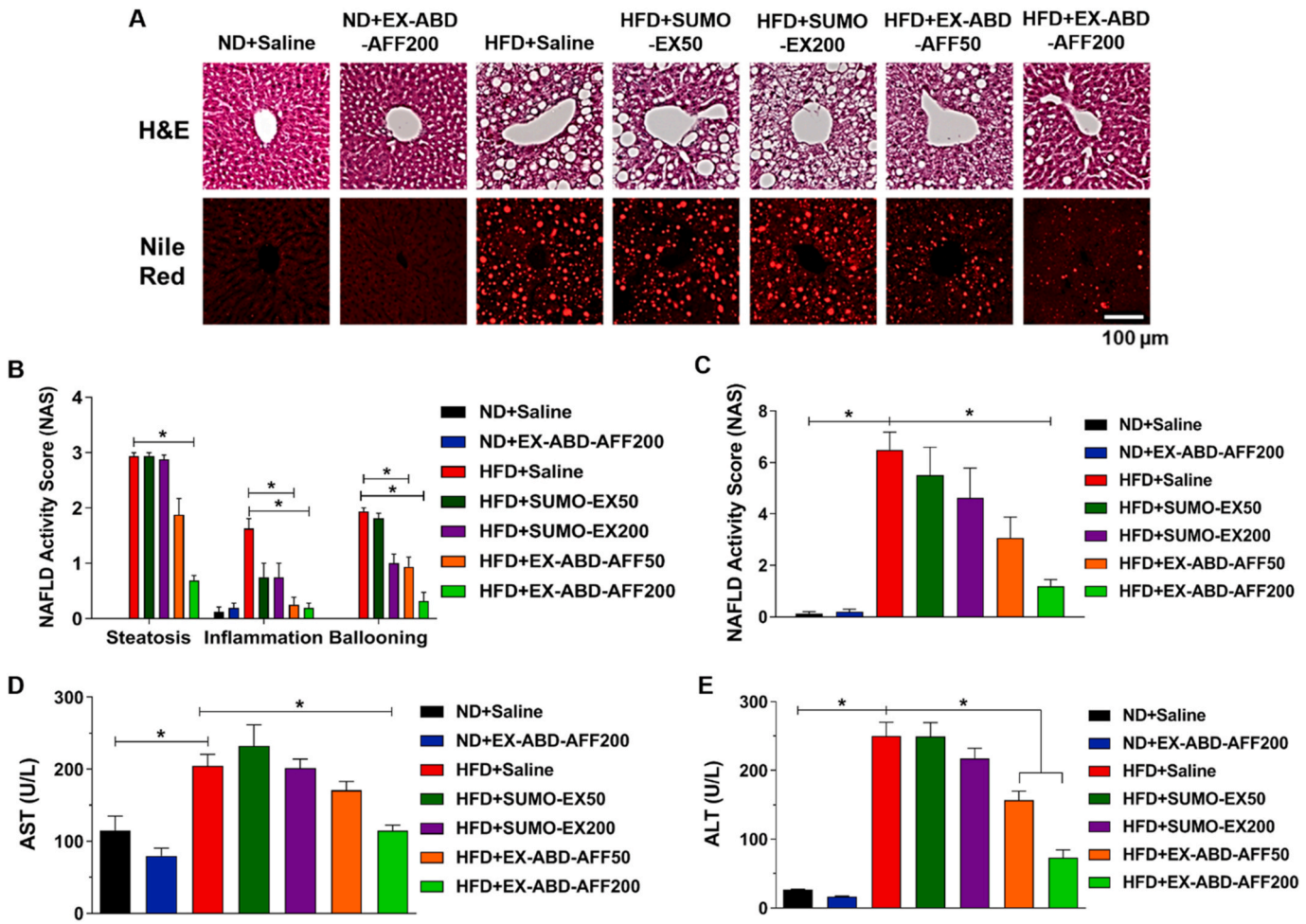

Fig. 7. Therapeutic effects of EX-ABD-AFF on non-alcoholic fatty liver disease (NAFLD) by long-term (10 weeks) treatment in high-fat diet (HFD)-fed C57/BL6 mice. (A) Representative histological images of the liver sections stained separately with H&E and Nile red. The red fluorescence in the Nile red-stained images show the accumulated fats. (B) Specific NAFLD activity scores (NAS) of steatosis, inflammation, and ballooning. (C) Total overall NAS. (D) Serum AST levels. (E) Serum ALT levels. The statistically significant difference in the body weight changes among the groups was compared by 1-way ANOVA and post hoc Tukey's multiple comparison test. *P < 0.05. (SUMO-EX: SUMO-tagged exendin-4, EX-ABD-AFF: SUMO-tagged exendin-4-albumin binding domain-anti-FcRn affibody fusion protein, AST: aspartate aminotransferase, ALT: alanine aminotransferase). (For interpretation of the references to color in this figure legend, the reader is referred to the Web version of this article.)

ABD-AFF, we conducted a Western blot assay for the proteins extracted from the hippocampus region of the brains. As shown in Fig. 8D–G, the Western blot assay results showed a significant increase of hippocampal EX-ABD-AFF and GLP-1R levels in both the EX-ABD-AFF-treated ND- and HFD-fed C57/BL6 mice. To further support the presence of EX-ABD-AFF in the hippocampus and the binding to GLP-1R, immunohistochemistry and a Duolink PLA assay were carried out. The results are shown in Figs. S9 and S10. Consistent with the Western blot results, stronger fluorescence intensities of both the anti-EX and anti-GLP-1R antibodies were observed from both the ND- and HFD-fed mice treated with EX-ABD-AFF (Fig. S9). Furthermore, duolink fluorescence signals, indicating EX-ABD-AFF and GLP-1R interaction, were more abundant in the hippocampal neurons of ND- and HFD-fed mice treated with the EX-ABD-AFF, compared to the saline-treated mice (Fig. S10). Overall, these results evidenced that the EX-ABD-AFF could distribute to the hippocampus region of the brain and directly act on activation of the GLP-1R.

4. Discussion

GLP-1, an incretin hormone released by intestinal L cells, has drawn great interest because of its therapeutic efficacy in the treatment of diabetes and metabolic complications of obesity that include elevated blood glucose, high triglycerides, and fatty liver [30]. These complications are further associated with an increased risk of developing type 2 diabetes and varied cardiovascular diseases [30]. Interestingly, GLP-1R agonists, including EX, share the major activities of GLP-1, such as stimulation of glucose-dependent insulin secretion and reduction of food intake [1,2,32,33]. As GLP-1R is expressed in many different organs such as pancreas (islet cells), liver, brain, and lung, the GLP-1R agonists could elicit varied therapeutic effects [33]. Thanks to extensive research efforts, the EX has become clinically approved for the treatment of diabetes. However, in spite of the great efficacy of EX, the pursuit for more effective GLP-1R agonists is yet ongoing, specifically because of the short plasma half-life of the EX which requires twice-daily administration [33]. To address this issue, in this research, we developed a novel super long-acting EX-fusion protein-coupled with ABD and AFF, named EX-ABD-AFF. The ABD was intended to enlarge the size of the fusion protein in the bloodstream to avoid rapid glomerular filtration, while the AFF enables the high-affinity binding to the endothelial FcRn for the FcRn-mediated recycling. In this research, the EX-ABD-AFF was expressed as a soluble and functional protein from the *E. coli* expression system with a high yield and could be successfully purified using Talon metal affinity chromatography (Fig. 2B and C).

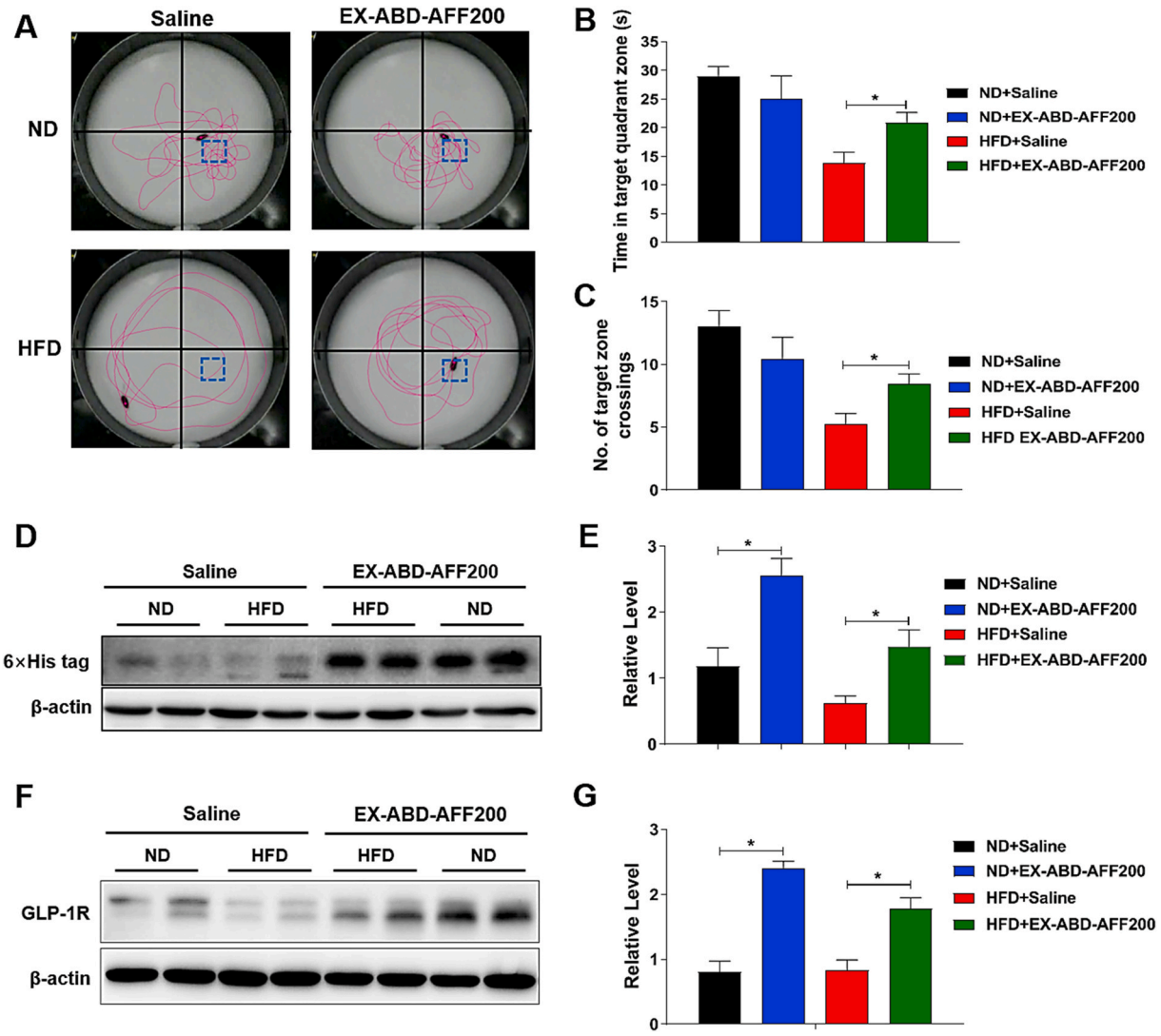

Fig. 8. Therapeutic effects of EX-ABD-AFF on improving cognitive deficits by long-term (10 weeks) treatment in high-fat diet (HFD)-fed C57/BL6 mice. (A) Representative swimming paths of the mice during the probe trial in Morris Water Maze (MWM) test. (B) Average time spent in the target zone and (C) number of target zone crossings of the mice in the MWM test. (D) Western blot results for hippocampal accumulation of EX-ABD-AFF. (E) Relative levels of EX-ABD-AFF. (F) Western blot results for hippocampal GLP-1R. (G) Quantitative analysis of the hippocampal GLP-1R levels. The statistically significant difference in the body weight changes among the groups was compared by 1-way ANOVA and post hoc Tukey's multiple comparison test. *P < 0.05. (EX-ABD-AFF: SUMO-tagged exendin-4-albumin binding domain-anti-FcRn affibody fusion protein).

After preparation, to verify the functionality of each component, the binding affinities of the produced EX-ABD-AFF to its expected targets were determined by surface plasmon resonance (SPR) analyses. The results showed that EX-ABD-AFF could indeed bind GLP-1R, HSA, and hFcRn with high binding affinities (Figs. S1A–S1C and Table 2). Notably, the binding of EX-ABD-AFF to the hFcRn was found pH-dependent (Figs. S1C and S1D) consistent to previous reports, and the affinity of the EX-ABD-AFF to the hFcRn (K_D: 83.2 nM at acidic condition) was similar to that of the AFF alone against hFcRn (K_D: 50 nM) reported by Seijsing et al. [22]. In comparison, with the identical SPR assay conditions applied for the binding of EX-ABD-AFF to hFcRn, no clear association/dissociation profiles were observed between HSA and the hFcRn up to 2 μM (data not shown). These results indicated that the EX-ABD-AFF possesses a higher binding affinity to the FcRn than albumin and albumin-bound EX-ABD.

After confirming the proper functionality of the EX-ABD-AFF, the feasibility of extending the plasma circulation time of EX by adopting the ABD-AFF fusion strategy was evaluated *in vivo*. Based on the obtained PK parameters (Fig. 3A and Table 3), it was found that the fusion of AFF alone could provide only a 2-fold extension for the plasma half-life of SUMO-EX (0.7 h). This may be explained by the small size of EX-AFF (MW: 24.9 kDa) and its inability to bind to the albumin. Generally, proteins or peptides smaller than the albumin (MW: 66.5 kDa for human albumin) are excreted rapidly [16]. Therefore, for a small peptide like EX, it would have been necessary to not only make it available for FcRn-mediated recycling, but also enlarge the size sufficient to avoid the rapid renal clearance [16]. In a sharp contrast, both the EX-ABD and EX-ABD-AFF showed markedly enhanced plasma circulation times than SUMO-EX (EX-ABD: 3.5 days and EX-ABD-AFF: 7 days); evidencing their successful albumin binding instantly after entering the bloodstream (Fig. 3B and Table 3). However, this will not be sufficient to explain all of the PK profiles, as the EX-ABD-AFF showed even a 2-fold longer plasma half-life and 5-fold greater AUC than the EX-ABD. When compared the plasma half-lives of the EX-ABD-AFF administered by *s.c. vs. i.v.*, it was further confirmed that the extension of the plasma half-life is surely because of the extension of the plasma circulation time rather than delayed absorption (Fig. 3B–C and Table 3). A possible explanation for longer plasma half-life of EX-ABD-AFF may be explained by two

aspects: 1) the unmatched binding affinity of the AFF to the FcRn, and 2) potentially synergistic binding of albumin (mediated through the ABD) and AFF together to the FcRn. Both the contributions may have rendered the EX-ABD-AFF to go through the FcRn-mediated recycling with the highest efficiency by winning the competition over endogenous antibodies and albumins abundantly present in the bloodstream [21]. Consistent to the PK data, the biodistribution of EX-ABD-AFF in the major organs (including brain, pancrease, and liver) were traceable up to 12 days (Figs. 3D and S3).

In the next step, the hypoglycemic activities of EXp, SUMO-EX, and EX-fusion proteins were assessed in HFD-fed mice. The short-term efficacy study results showed similar effects by EXp and the SUMO-EX, in spite of significant difference in their potency for activiation of the GLP-1R (Figs. S2 and 4B). However, compared with the SUMO-EX, there were marked differences in the duration of hypoglycemic effects by the EX-fusion proteins (Fig. 4C). While the blood-glucose-lowering effects lasted for only 6 h for EX-AFF (similar to SUMO-EX) and, 3 days for EX-ABD and EX-ABD-controlAFF, notably, dose-dependent hypoglycemic effects were observed from the EX-ABD-AFF-treated mice for over 12 days (Fig. 4C and S4B–S4C). These data well correlated to the PK study results (Fig. 3A–C and Table 3); strongly suggesting that extending the plasma half-life may be the critical factor for the prolonged hypoglycemic effects [34]. Furthermore, the data evidenced again the superiority of the ABD-AFF fusion strategy over other conventional approaches (such as adopting only the ABD). Another finding from the short-term efficacy study was that the EX-ABD-AFF could significantly decrease the bodyweight of the HFD-fed mice for 12 days even with a single administration; presumably by suppressing their food intake (Figs. 4D and S4D). These results suggested that indeed the EX-ABD-AFF could not only provide extended glycemic control but may also be effective in the treatment of obesity and related complications [35,36].

Encouraged by the short-term efficacy study results, the therapeutic benefits of the EX-ABD-AFF in the treatment of obesity and related metabolic (hyperglycemia, hyperlipidemia, and NAFLD) and cognitive complications were evaluated in a long-term (10-week) study. The first finding from the long-term study was that, in HFD-fed mice, the EX-ABD-AFF could elicit significant hypoglycemic effects and furthermore provide improvement of glucose tolerance and insulin resistance. However, the glucose-lowering effects were not observed from the ND-fed mice (Fig. 5A and B); suggesting that the EX-ABD-AFF may have a low risk of causing hypoglycemia shock in non-hyperglycemic condition. These results were in good agreement with the previous report that the insulinotropic action of GLP-1 is glucose-dependent (i.e., insulin secretion requires a rise of glucose to a certain level [35]).

To verify the mechanism for these hypoglycemic effects, when the pancreas sections and the serum insulin levels were examined, we could find direct evidence of the pancreatic delivery of the EX-ABD-AFF (Fig. 6A and B), and furthermore, observe the largest insulin-positive area (indicating the β-cell area) (Fig. 6C) and the highest serum insulin level (Fig. 6E) from the HFD + EX-ABD-AFF200-treated group. These results suggested that the hypoglycemic effects of EX-ABD-AFF were elicited by its insulinotropic activity. Furthermore, it was also notified that indeed the EX-ABD-AFF could increase the β-cell mass (Fig. S6) presumably by stimulation of neogenesis and proliferation of β-cells, and suppression of their apoptosis [32].

Second, the EX-ABD-AFF could provide a reduction of body weight. The body weights of the EX-ABD-AFF-treated HFD-fed mice maintained lower than the HFD + Saline mice (maximally 17% reduction at week 4 and 13% at week 10) (Fig. 5C). In good correlation, compared with the HFD + Saline group, the food intake amounts of the HFD + EX-ABD-AFF200 group were also significantly reduced; confirming the possible link between the decrease of appetite and the body weight loss (Fig. 5D). According to Edwards et al., the infusion of EX to healthy human volunteers caused a delay in gastric emptying and a reduction in food intake [37]. Regarding the underlying mechanism, Kanoski et al. reported that EX could suppress the food intake by activation of the GLP-1R expressed on vagal afferent fibers innervating the stomach and small intestine [38]. Mediated by inhibitory vagus nerves, the EX attenuates meal-induced antral propagated contractions as well as enhances the pyloric tone of the stomach, which eventually leads to delayed gastric emptying [38,39]. In addition, the EX has been known to induce the loss of appetite by acting upon the hypothalamus which controls the appetite and food intake through various mechanisms mediated by the GLP-1Rs [40]. . Overall, the anorexic effects induced by the EX-ABD-AFF are likely explained by the combination of these central and peripheral effects [35].

Third, the EX-ABD-AFF could elicit hypolipidemic effects. In the EX-ABD-AFF-treated HFD-fed mice, a significant reduction was observed for total fats, serum FFA and serum TG concentrations compared with the HFD control mice (Figs. S7A–S7D). Furthermore, it was also effective in the treatment of NAFLD (Figs. 7 and S8). This improvement in the NAFLD conditions is likely the consequence of systemic reduction of the whole body fat as well as direct hepatic actions of the EX-ABD-AFF (*via* binding to the GLP-1R on liver cells). In this regard, Lee et al. proposed that GLP-1R agonists may ameliorate the NAFLD by improving hepatic glucose metabolism, increasing fatty acid oxidation, and decreasing lipogenesis [30].

Lastly, the EX-ABD-AFF was found effective in improving the cognitive dysfunction. The hippocampus is the brain region that is crucial for learning and memory [41,42]. The hippocampal cells have expression of GLP-1R, and the significant contribution of the interplay among the GLP-1R and the GLP-1R agonists on the cognitive function of the hippocampus have been demonstrated by previous studies. Oka et al. reported that GLP-1 could modulate neuronal activity in the rat hippocampus *via* the activation of GLP-1R [43]. Abbas et al. further reported that the GLP-1R knockout mice were characterized with possessing impaired long-term potentiation (LTP) in the hippocampus [44]. However, the learning ability of the GLP-1R deficient mice could be restored by hippocampal glp1r gene transfer [45]. Also, notably, Bomba et al. reported that EX could reverse the HFD-induced impairment of brain-derived neurotrophic factor signaling and neuroinflammation in 3 × Tg-Alzheimer's disease mice challenged with a HFD [46]. Consistent with the previous reports, the MWM test results clearly showed a reversal of cognitive deficits in EX-ABD-AFF-treated HFD mice (Fig. 8A–C). Based on the Western blot assay results (Fig. 8D–G), this improvement in the cognitive deficits may be explained by activation of the hippocampal GLP-1R by the EX-ABD-AFF; as evidenced by the significantly elevated levels of hippocampal EX-ABD-AFF and GLP-1R levels in the EX-ABD-AFF-treated mice. Through the Western blot assay (using the anti-His-tag antibody) (Fig. 8D–E), immunofluorescence (Fig. S9), and the Duolink immunofluorescence (Fig. S10) results, notably, we could find evidences that the EX-ABD-AFF could be indeed delivered to the hippocampus of the brain and further bind to the hippocampal GLP-1R. Because the EX-ABD-AFF was also observed in the hippocampus of ND-fed mice (Fig. 8D and E, S9, and S10), this brain delivery of EX-ABD-AFF may not be the consequence of a defect in the BBB that are often found in the diabetic mice models [47]. How the EX-ABD-AFF could penetrate the BBB is, however, yet to be resolved.

The potential immunogenicity issue is of great concern for commonly all the therapeutic proteins and peptides. Especially, as both the ABD and AFF are derived from bacterial origin (streptococcal protein G and Z domain of the Staphylococcal protein A, respectively), the immunogenicity issue cannot be neglected for the EX-ABD-AFF [24,25]. To this regard, Nilvebrant et al. previously reported bacterial proteins used to have evolved to mediate immune escape, thus tend to have low immunogenicity [48]. In addition, the modification of proteins with PEGylation or albumin fusion has also been proven to reduce the immunogenicity by physically masking their surface [49]. Specifically, regarding the affibody, it has already been proven lack of toxicity and immunogenicity through preclinical and clinical studies [50,51]. However, for the ABD, information of the immunogenicity yet lacks. Therefore, along with assessment of the safety, the immunogenicity of

EX-ABD-AFF would definitely be included in our further studies and, to minimize these concerns, we would attempt various strategies, such as substitution of the ABD to less immunogenic ones. Despite the potential safety and immunogenicity issues remaining to be evaluated, overall, the results of this research clearly demonstrated that the EX-ABD-AFF possesses a high potency in the treatment of obesity and obesity-related metabolic and cognitive complications.

5. Conclusion

This is the first report of the application of a combination of ABD and AFF fusion strategy to extend the plasma half-life of a therapeutically active protein. Specifically, in this research, we applied this strategy to develop a super long-lasting EX-fusion protein, "EX-ABD-AFF". By the synergistic effects of "ABD-induced efficient serum albumin binding" and "AFF-mediated high-affinity binding to FcRn", the EX-ABD-AFF could have a super-long plasma half-life of 7 days which is, to date, the longest among all the reported EX analogs. This remarkably extended duration of the plasma circulation and an 821-fold higher plasma exposure than the SUMO-EX enabled the EX-ABD-AFF to provide significant hypoglycemic effects in the HFD-fed mice for over 12 days. More importantly, the EX-ABD-AFF could also reduce the bodyweights, fat contents, and improve the NAFLD conditions in the HFD-fed mice. Furthermore, the EX-ABD-AFF could be delivered to the hippocampus region of the brain and could reverse cognitive deficits. All these study results strongly support that the EX-ABD-AFF possesses a great potential to become an effective agent for not only the treatment of type 2 diabetes but also the underlying obesity and obesity-related metabolic and cognitive complications. Overall, this study demonstrated that the ABD-AFF fusion could serve as an effective strategy to highly extend the plasma half-lives of therapeutic proteins, and thereby provide significantly prolonged and greater therapeutic effects.

Author contributions

M.C.S. and G.S.R., conceptualization, supervision, resources, and writing-original draft preparation and review; J.Y.L., T.P., R.A., and K. P., investigation, methodology, data curation, formal analysis; J.Y.L., T. P., K.A.M., G.S.R., and M.C.S. writing-review and editing; E.H. and Y.H. P., data curation, validation and formal analysis; K.A.M., M.J., S.L., and S.H., investigation and methodology; G.S.R., M.C.S., and K.A.M., funding acquisition and project administration. All authors approved the final version of the manuscript.

Data availability

The raw/processed data required to reproduce these findings cannot be shared at this time due to technical or time limitations.

Declaration of competing interest

The authors declare no competing financial interest.

Acknowledgments

This work was financially supported by grants from the Basic Science Research Program through the National Research Foundation of Korea (NRF) funded by the Ministry of Education, Science and Technology (NRF-2015R1A5A2008833, NRF-2018R1D1A1A02047809, and NRF-2018R1D1A1B07048818).

Appendix A. Supplementary data

Supplementary data to this article can be found online at https://doi.org/10.1016/j.biomaterials.2020.120250.

References

[1] J.P. Raufman, Bioactive peptides from lizard venoms, Regul. Pept. 61 (1) (1996) 1–18.
[2] B.L. Furman, The development of Byetta (exenatide) from the venom of the Gila monster as an anti-diabetic agent, Toxicon 59 (4) (2012) 464–471.
[3] P. Shrestha, S. Regmi, J.-H. Jeong, Injectable hydrogels for islet transplantation: a concise review, J. Pharm. Investig. 50 (2020) 29–45.
[4] D. Tang, H. Tian, J. Wu, J. Cheng, C. Luo, W. Sai, X. Song, X. Gao, W. Yao, C-terminal site-specific PEGylated Exendin-4 analog: a long-acting glucagon like Peptide-1 receptor agonist, on glycemic control and beta cell function in diabetic db/db mice, J. Pharmacol. Sci. 138 (1) (2018) 23–30.
[5] S.H. Lee, S. Lee, Y.S. Youn, D.H. Na, S.Y. Chae, Y. Byun, K.C. Lee, Synthesis, characterization, and pharmacokinetic studies of PEGylated glucagon-like peptide-1, Bioconjugate Chem. 16 (2) (2005) 377–382.
[6] X. Zhong, S. Yang, T. Liu, S. Ji, J. Hu, H. Li, Engineering a novel protease-based Exendin-4 derivative for type 2 antidiabetic therapeutics, Eur. J. Med. Chem. 150 (2018) 841–850.
[7] O.E. Levy, C.M. Jodka, S.S. Ren, L. Mamedova, A. Sharma, M. Samant, L. J. D'Souza, C.J. Soares, D.R. Yuskin, L.J. Jin, D.G. Parkes, K. Tatarkiewicz, S. S. Ghosh, Novel exenatide analogs with peptidic albumin binding domains: potent anti-diabetic agents with extended duration of action, PloS One 9 (2) (2014), e87704.
[8] L. Zhang, L. Wang, Z. Meng, H. Gan, R. Gu, Z. Wu, L. Gao, X. Zhu, W. Sun, J. Li, Y. Zheng, G. Dou, A novel exendin-4 human serum albumin fusion protein, E2HSA, with an extended half-life and good glucoregulatory effect in healthy rhesus monkeys, Biochem. Biophys. Res. Commun. 445 (2) (2014) 511–516.
[9] J.H. Kong, E.J. Oh, S.Y. Chae, K.C. Lee, S.K. Hahn, Long acting hyaluronate–exendin 4 conjugate for the treatment of type 2 diabetes, Biomaterials 31 (14) (2010) 4121–4128.
[10] K. Li, L. Yu, X. Liu, C. Chen, Q. Chen, J. Ding, A long-acting formulation of a polypeptide drug exenatide in treatment of diabetes using an injectable block copolymer hydrogel, Biomaterials 34 (11) (2013) 2834–2842.
[11] J. Lee, C. Lee, T.H. Kim, E.S. Lee, B.S. Shin, S.C. Chi, E.S. Park, K.C. Lee, Y.S. Youn, Self-assembled glycol chitosan nanogels containing palmityl-acylated exendin-4 peptide as a long-acting anti-diabetic inhalation system, J. Contr. Release 161 (3) (2012) 728–734.
[12] J.S. Geiser, M.A. Heathman, X. Cui, J. Martin, C. Loghin, J.Y. Chien, A. de la Peña, Clinical pharmacokinetics of dulaglutide in patients with type 2 diabetes: analyses of data from clinical trials, Clin. Pharmacokinet. 55 (5) (2016) 625–634.
[13] J.E. Matthews, M.W. Stewart, E.H. De Boever, R.L. Dobbins, R.J. Hodge, S. E. Walker, M.C. Holland, M.A. Bush, Pharmacodynamics, pharmacokinetics, safety, and tolerability of albiglutide, a long-acting glucagon-like peptide-1 mimetic, in patients with type 2 diabetes, J. Clin. Endocrinol. Metab. 93 (12) (2008) 4810–4817.
[14] K.B. Sutradhar, S. Khatun, A. Al Mamun, M. Begum, Distribution and elimination of protein therapeutics: a review, Stamford J. Pharm. Sci. 4 (2) (2011) 1–12.
[15] M.A. Tabrizi, C.M. Tseng, L.K. Roskos, Elimination mechanisms of therapeutic monoclonal antibodies, Drug Discov, Today Off. 11 (1–2) (2006) 81–88.
[16] T. Maack, V. Johnson, S.T. Kau, J. Figueiredo, D. Sigulem, Renal filtration, transport, and metabolism of low-molecular-weight proteins: a review, Kidney Int. 16 (3) (1979) 251–270.
[17] R.E. Kontermann, Strategies for extended serum half-life of protein therapeutics, Curr. Opin. Biotechnol. 22 (6) (2011) 868–876.
[18] R. Zaman, R.A. Islam, N. Ibnat, I. Othman, A. Zaini, C.Y. Lee, E.H. Chowdhury, Current strategies in extending half-lives of therapeutic proteins, J. Contr. Release 301 (2019) 176–189.
[19] W.Y. Lee, M. Asadujjaman, J.-P. Jee, Long acting injectable formulations: the state of the arts and challenges of poly (lactic-co-glycolic acid) microsphere, hydrogel, organogel and liquid crystal, J. Pharm. Investig. 49 (2019) 459–476.
[20] D. Sleep, J. Cameron, L.R. Evans, Albumin as a versatile platform for drug half-life extension, Biochim. Biophys. Acta 1830 (12) (2013) 5526–5534.
[21] K.M.K. Sand, M. Bern, J. Nilsen, H.T. Noordzij, I. Sandlie, J.T. Andersen, Unraveling the interaction between FcRn and albumin: opportunities for design of albumin-based therapeutics, Front. Immunol. 5 (2015) 682.
[22] J. Seijsing, M. Lindborg, I. Hoiden-Guthenberg, H. Bonisch, E. Guneriusson, F. Y. Frejd, L. Abrahmsen, C. Ekblad, J. Lofblom, M. Uhlen, T. Graslund, An engineered affibody molecule with pH-dependent binding to FcRn mediates extended circulatory half-life of a fusion protein, Proc. Natl. Acad. Sci. U.S.A. 111 (48) (2014) 17110–17115.
[23] S.A. Jacobs, A.C. Gibbs, M. Conk, F. Yi, D. Maguire, C. Kane, K.T. O'Neil, Fusion to a highly stable consensus albumin binding domain allows for tunable pharmacokinetics, Protein Eng. Des. Sel. 28 (10) (2015) 385–393.
[24] B. Akerström, E. Nielsen, L. Björck, Definition of IgG-and albumin-binding regions of streptococcal protein G, J. Biol. Chem. 262 (28) (1987) 13388–13391.
[25] K. Nord, E. Gunneriusson, J. Ringdahl, S. Ståhl, M. Uhlén, P.-Å. Nygren, Binding proteins selected from combinatorial libraries of an α-helical bacterial receptor domain, Nat. Biotechnol. 15 (8) (1997) 772–777.
[26] J. Lofblom, J. Feldwisch, V. Tolmachev, J. Carlsson, S. Stahl, F.Y. Frejd, Affibody molecules: engineered proteins for therapeutic, diagnostic and biotechnological applications, FEBS Lett. 584 (12) (2010) 2670–2680.
[27] V. Tolmachev, F.Y. Nilsson, C. Widström, K. Andersson, D. Rosik, L. Gedda, A. Wennborg, A.J. Orlova, 111In-benzyl-DTPA–ZHER2: 342, an affibody-based conjugate for in vivo imaging of HER2 expression in malignant tumors, J. Nucl. Med. 47 (5) (2006) 846–853.

[28] C. Monton, P. Kulvanich, Characterization of crosslinked hard gelatin capsules for a structural assembly of elementary osmotic pump delivery system, J. Pharm. Investig. 49 (6) (2019) 655–665.
[29] B.T. Jeon, E.A. Jeong, H.J. Shin, Y. Lee, D.H. Lee, H.J. Kim, S.S. Kang, G.J. Cho, W. S. Choi, G.S. Roh, Resveratrol attenuates obesity-associated peripheral and central inflammation and improves memory deficit in mice fed a high-fat diet, Diabetes 61 (6) (2012) 1444–1454.
[30] J. Lee, S.W. Hong, E.J. Rhee, W.Y. Lee, GLP-1 receptor agonist and non-alcoholic fatty liver disease, Diabetes Metab. J. 36 (4) (2012) 262–267.
[31] C.V. Vorhees, M.T. Williams, Morris water maze: procedures for assessing spatial and related forms of learning and memory, Nat. Protoc. 1 (2) (2006) 848–858.
[32] L.L. Nielsen, A.A. Young, D.G. Parkes, Pharmacology of exenatide (synthetic exendin-4): a potential therapeutic for improved glycemic control of type 2 diabetes, Regul. Pept. 117 (2) (2004) 77–88.
[33] A. Lund, F.K. Knop, T. Vilsboll, Emerging GLP-1 receptor agonists, Expet Opin. Emerg. Drugs 16 (4) (2011) 607–618.
[34] D.-G. Han, S.-S. Cho, J.-H. Kwak, I.-S. Yoon, Medicinal plants and phytochemicals for diabetes mellitus: pharmacokinetic characteristics and herb-drug interactions, J. Pharm. Investig. 49 (2019) 603–612.
[35] D.P. Bradley, R. Kulstad, D.A. Schoeller, Exenatide and weight loss, Nutrition 26 (3) (2010) 243–249.
[36] J. Li, R. Cha, H. Luo, W. Hao, Y. Zhang, X. Jiang, Nanomaterials for the theranostics of obesity, Biomaterials 223 (2019) 119474.
[37] C.M. Edwards, S.A. Stanley, R. Davis, A.E. Brynes, G.S. Frost, L.J. Seal, M.A. Ghatei, S.R. Bloom, Exendin-4 reduces fasting and postprandial glucose and decreases energy intake in healthy volunteers, Am. J. Physiol. Endocrinol. Metab. 281 (1) (2001) E155–E161.
[38] S.E. Kanoski, S.M. Fortin, M. Arnold, H.J. Grill, M.R. Hayes, Peripheral and central GLP-1 receptor populations mediate the anorectic effects of peripherally administered GLP-1 receptor agonists, liraglutide and exendin-4, Endocrinol 152 (8) (2011) 3103–3112.
[39] N.e. I. meryüz, B.C. Yegen, A. Bozkurt, T. Coskun, M.L. Villanueva-Penacarrillo, N. B. Ulusoy, Glucagon-like peptide-1 inhibits gastric emptying via vagal afferent-mediated central mechanisms, Am. J. Physiol. Gastrointest. Liver Physiol. 273 (4) (1997) G920–G927.
[40] S.L. Dickson, R.H. Shirazi, C. Hansson, F. Bergquist, H. Nissbrandt, K.P. Skibicka, The glucagon-like peptide 1 (GLP-1) analogue, exendin-4, decreases the rewarding value of food: a new role for mesolimbic GLP-1 receptors, J. Neurosci. 32 (14) (2012) 4812–4820.
[41] A.J. Kastin, V. Akerstrom, W. Pan, Interactions of glucagon-like peptide-1 (GLP-1) with the blood-brain barrier, J. Mol. Neurosci. 18 (1–2) (2002) 7–14.
[42] A. Kastin, V. Akerstrom, Entry of exendin-4 into brain is rapid but may be limited at high doses, Int. J. Obes. 27 (3) (2003) 313–318.
[43] J.-I. Oka, N. Goto, T. Kameyama, Glucagon-like peptide-1 modulates neuronal activity in the rat's hippocampus, Neuroreport 10 (8) (1999) 1643–1646.
[44] T. Abbas, E. Faivre, C. Hölscher, Impairment of synaptic plasticity and memory formation in GLP-1 receptor KO mice: interaction between type 2 diabetes and Alzheimer's disease, Behav. Brain Res. 205 (1) (2009) 265–271.
[45] M.J. During, L. Cao, D.S. Zuzga, J.S. Francis, H.L. Fitzsimons, X. Jiao, R.J. Bland, M. Klugmann, W.A. Banks, D.J. Drucker, C.N. Haile, Glucagon-like peptide-1 receptor is involved in learning and neuroprotection, Nat. Med. 9 (9) (2003) 1173–1179.
[46] M. Bomba, A. Granzotto, V. Castelli, M. Onofrj, R. Lattanzio, A. Cimini, S.L. Sensi, Exenatide reverts the high-fat-diet-induced impairment of BDNF signaling and inflammatory response in an animal model of Alzheimer's disease, J. Alzheim. Dis. 70 (3) (2019) 793–810.
[47] H.C. Chang, Y.T. Tai, Y.G. Cherng, J.W. Lin, S.H. Liu, T.L. Chen, R.M. Chen, Resveratrol attenuates high-fat diet-induced disruption of the blood-brain barrier and protects brain neurons from apoptotic insults, J. Agric. Food Chem. 62 (15) (2014) 3466–3475.
[48] J. Nilvebrant, S. Hober, The albumin-binding domain as a scaffold for protein engineering, Comput. Struct. Biotechnol. J. 6 (7) (2013), e201303009.
[49] I. Kim, T.H. Kim, K. Ma, E.-S. Park, K.T. Oh, E.S. Lee, K.C. Lee, Y.S. Youn, A 4-arm polyethylene glycol derivative conjugated with exendin-4 peptide and palmitylamine having dual-function of size-increase and albumin-binding for long hypoglycemic action, Regul. Pept. 167 (2–3) (2011) 239–245.
[50] H. Honarvar, K. Westerlund, M. Altai, M. Sandström, A. Orlova, V. Tolmachev, A. E. Karlström, Feasibility of affibody molecule-based PNA-mediated radionuclide pretargeting of malignant tumors, Theranostics 6 (1) (2016) 93–103.
[51] K. Westerlund, M. Altai, B. Mitran, M. Konijnenberg, M. Oroujeni, C. Atterby, M. de Jong, A. Orlova, J. Mattsson, P. Micke, A.E. Karlstrom, V. Tolmachev, Radionuclide therapy of HER2-expressing human xenografts using affibody-based peptide nucleic acid–mediated pretargeting: in vivo proof of principle, J. Nucl. Med. 59 (7) (2018) 1092–1098.